Theory and Practice of Wet Spinning of Cellulose Solutions

Doctoral Course, Part 1 & 2

Aalto University
School of Chemical
Engineering

Herbert Sixta

March 10 – 11, 2022

Outline

1. Introduction, history
2. Pulp as raw material
3. Cellulose solvents
4. Aspects of cellulose dissolution
5. Rheology of cellulose solutions
6. Coagulation and regeneration of cellulose
7. Filament breaches during spinning
8. Types of MMCFs
9. Properties of MMCFs

Schedule

L1	Introduction, Raw material	March 10	9:00 – 9:45
L2	Raw materials. Cellulose solvent	March 10	10:00-10:45
L3	Cellulose solvents	March 10	11:00-11:45
L4	Cellulose solvents	March 10	12:00-12:45
	Break		
L5	Cellulose dissolution	March 10	14:00-14:45
L6	Rheology	March 10	15:00-15:45
L7	Cellulose dissolution/ Coagulation and Regeneration	March 10	16:00-16:45
L8	Coagulation and Regeneration	March 11	9:00 – 9:45
L9	Coagulation and Regeneration	March 11	10:00-10:45
L10	Filament breaches	March 11	11:00-11:45
L11	Types and properties of MMCFs	March 11	12:00-12:45
L12	Q&A	March 11	13:00 -

1

Introduction, history

How to make Cellulose Fibers?

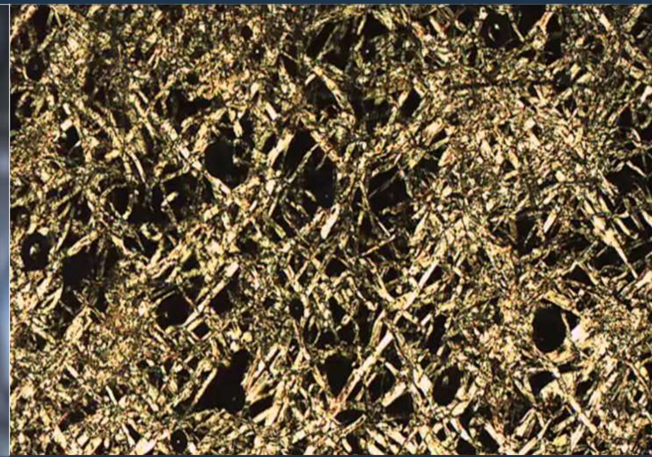

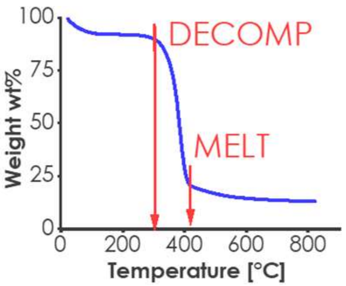

NOT MELTABLE

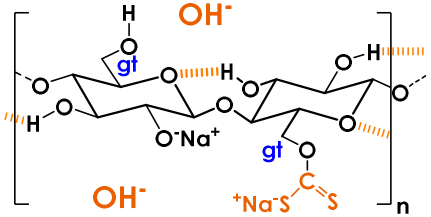

cellulose xanthate

VISCOSE

DIRECT DISSOLUTION

LYOCELL

Lýein = dissolve

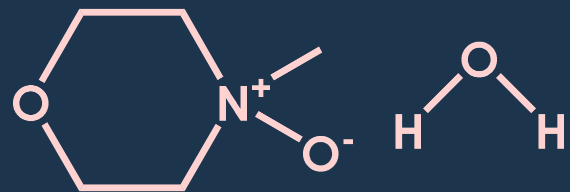

N-methylmorpholine-N-oxide

HISTORY

of

MAN-MADE CELLULOSE FIBERS

Cellulose nitrate

Nitration with nitric / sulfuric acid dissolution in EtOH and ether Dry-spinning. Denitration in $(NH_4)_2S$

Year	event
1845	C-F. Schöbein
1883	J-W Swan, commercial.
1889	Chardonnet World exhibition in Paris
1891	Denitration
1900	Many start-ups
1910	Closures, CV better alternative
1935	Last closure

Cupro

Cuprammonium rayon

Dissolution in $[Cu(NH_3)_4(H_2O)](OH)_2$ Wet spinning in water / sulfuric acid

Year	event
1857	Schweizer
1890	Despaissis technical application
1899	Fremery&Urban first textile fibers
1901	Bemberg (Thiele) stretch spinning
1931	Asahi Kasei operation in Japan
1980	Stop of fiber production in Germany
2015	Asahi Kasei expanded to 17 kt/a
2021	Production ongoing

Viscose (CV, CMD)

Alkalization, xanthation, dissolution in NaOH, wet spinning in aqueous Sulfuric acid, Na_2SO_4, $ZnSO_4$

Year	event
1892	Cross, Bevan Beadle (GB 8700)
1899	Cross&Stearn, viscose syndicate
1904	Courtauld Conventry production
1916	Oberbruch, Germ. First staple fiber
1931	Lilienfeld fiber 60 cN/tex
1943	Polynosic (Toramomen)
1950	Cox, first modifier, cotton-like, Supercord
1965	Modal fiber
1985	Mill closure (CS_2, H_2S, wastewater)
1985	Closures in Europe
2004	Polynosic stops
2021	CV+CMD: 6.5 Mt/a

Lyocell (CLY)

Direct solvent. Dry-jet Wet Spinning

Year	event
1939	**Graenacher:** tert-amine oxide US 2,179,181
1969	**Kodak,** Johnson, D.L.: US 3,447,939
1969	American Enka piloting; 1979 stop
1979	Courtauld started
1983	Lenzing started
1989	New Generic name – Lyocell (CLY)
1992	Mobile, USA, Courtauld 1st plant
1997	Heiligenkreuz, Lenzing 1st plant
2005	Lenzing acquires Tencel group
2014	4 Lyocell plants by Lenzing
2021	~270 kt/a Lenzing ~100 kt/a China

Global Fiber Market 2019

- 65% Synthetics, CAGR = 3.8%
- Natural fibers stagnating
- Cellulosics, CAGR = 3.8%

Fiber Year 2020

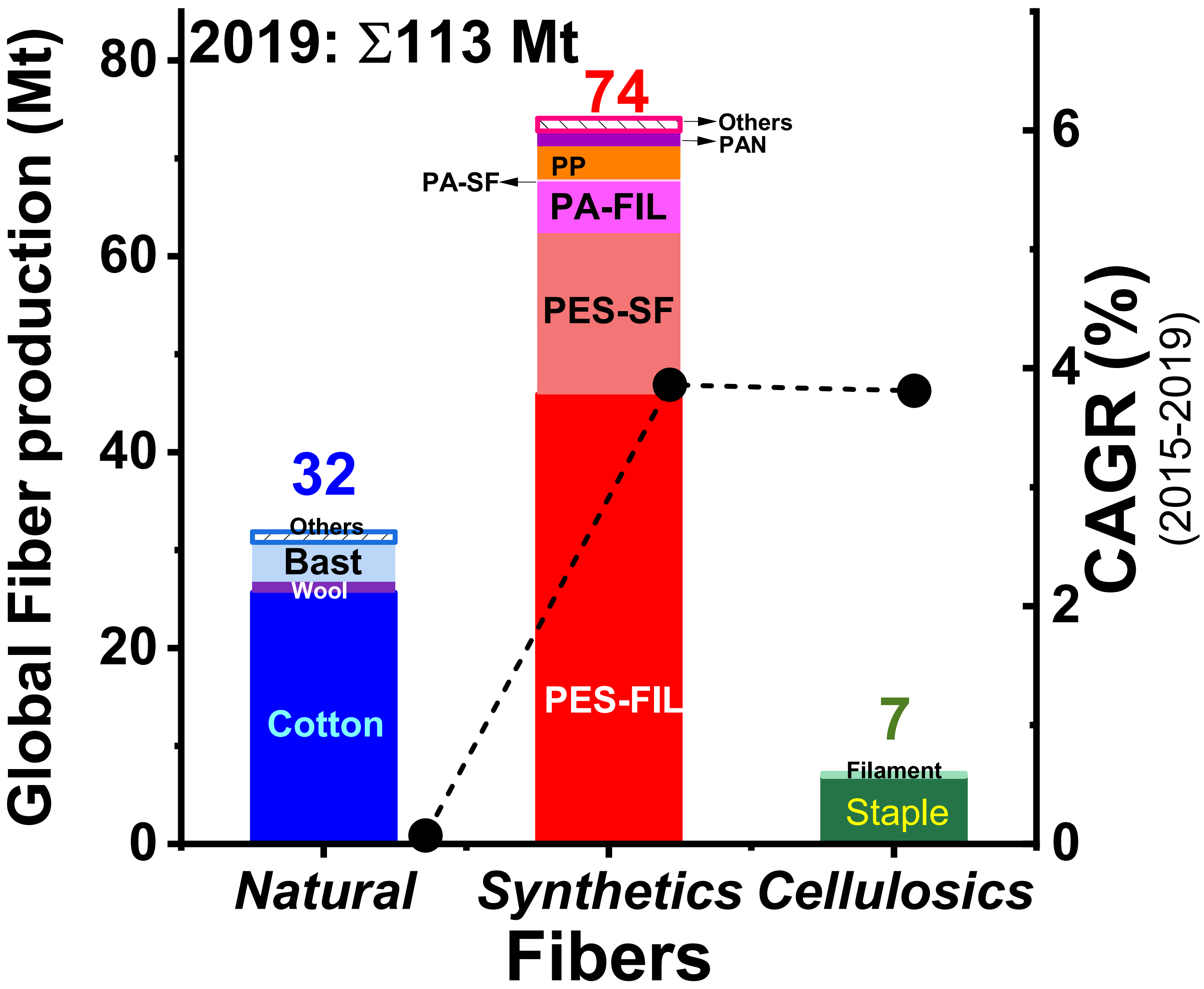

BISFA

Definition of Man-made Cellulose Fibers

Viscose	CV
Modal	CMD
Cupro	CUP
Lyocell	CLY
Cellulose acetate	CA
Cellulose triacetate	CTA

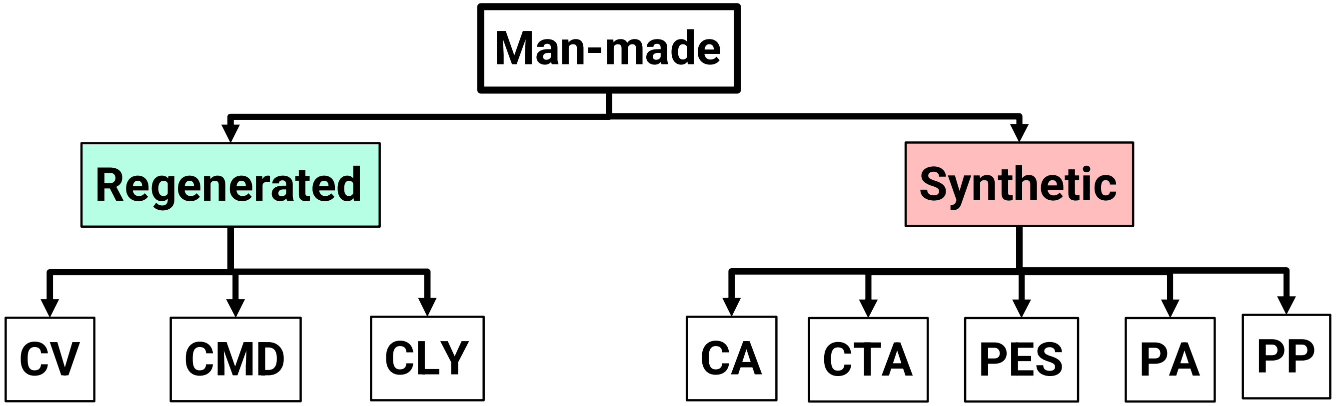

Life Cycle Assessment of Man-Made Cellulose Fibers

LCA Single Score Analysis cradle-to-factory gate

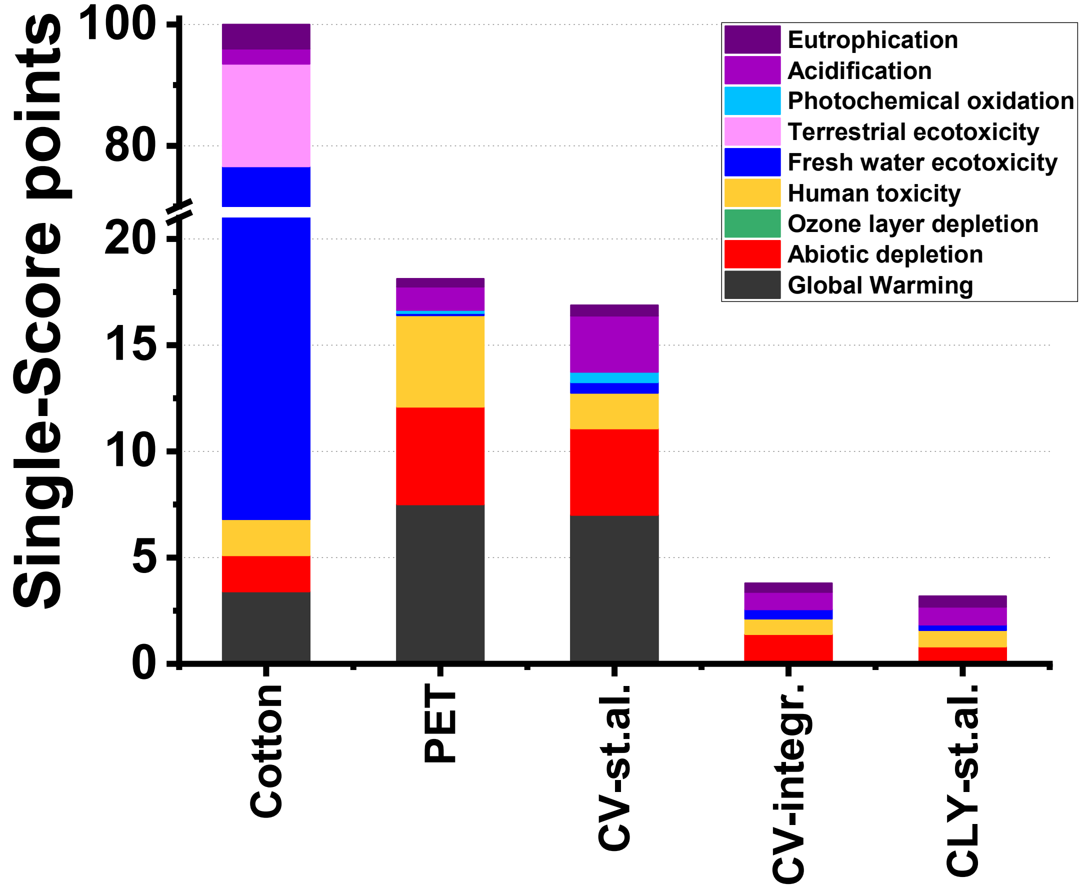

Li Shen and Martin K Patel, Lenz Ber (2010), 88, 1-59; 60-66

Ambition 1

Elimination of substances of concern, and microplastic emission

Ellen MacArthur Foundation's widely acclaimed report (2017)

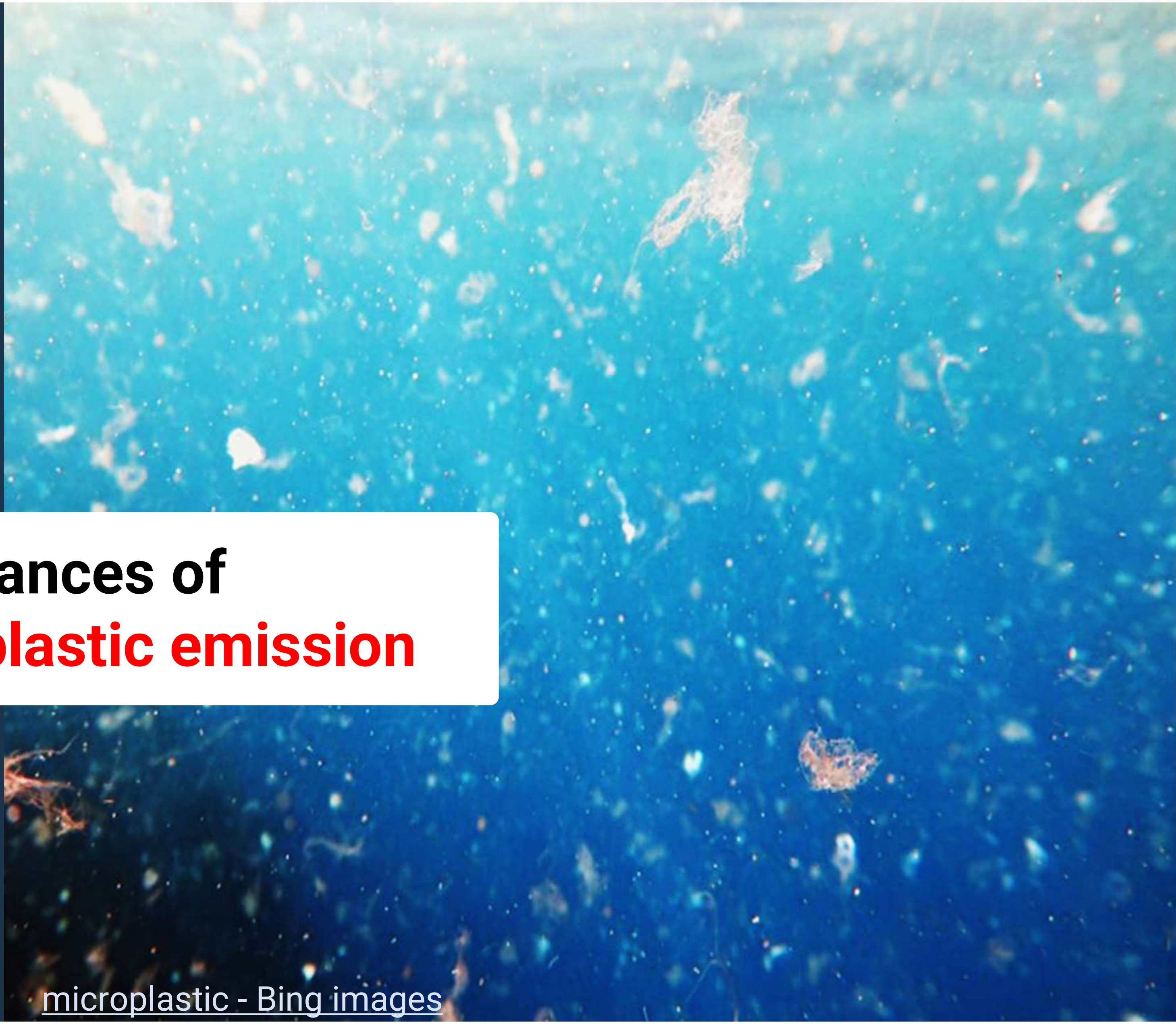

microplastic - Bing images

Global Plastic emissions

380 Mt/a Production
58% enter environment

Geyer, R. et al. Sci. Adv. 2017, 3 (7), No. e1700782

19–23 Mt of plastic waste entered aquatic ecosystem in 2016 (6% of Σ)

Borrelle et al., Science 369, 1515–1518 (2020

0.12-0.31 kg MF/ MP released per ton of washed fabric

Scientific Reports | (2019) 9:6633

Predicted growth in plastic waste entered aquatic ecosystems

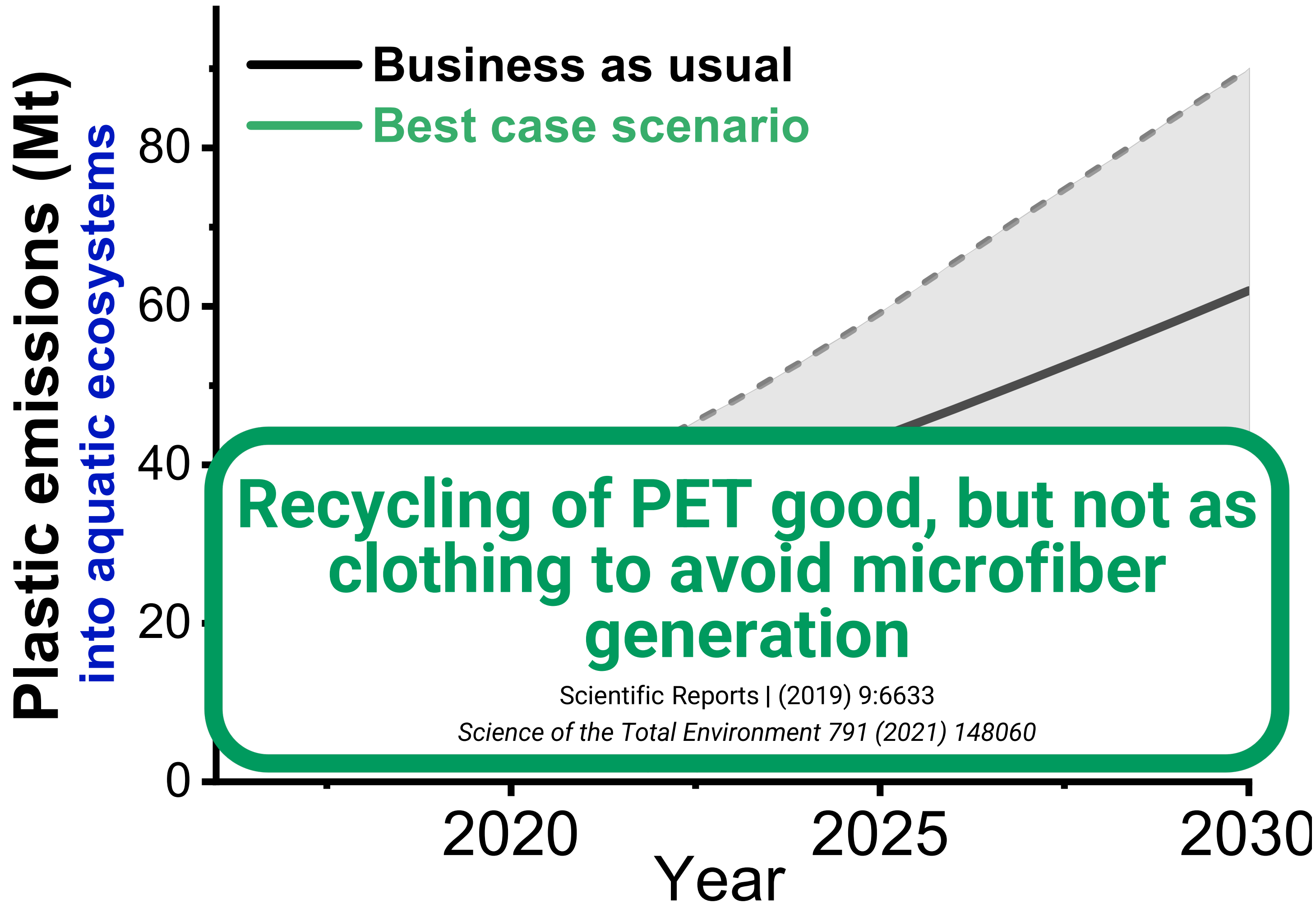

Recycling of PET good, but not as clothing to avoid microfiber generation

Scientific Reports | (2019) 9:6633

Science of the Total Environment 791 (2021) 148060

Best case scenario: Reductions related to 2016

(a) Bans on SUP
-25 to - 40 % (LI vs HI)

(b) Proportion waste managed:
66 to 99% (LI vs HI)

(c) Proportion recovered:
All countries: 40 %


Image: Pixabay

Borrelle et al., Science 369, 1515–1518 (2020)

Deconstruction of material swatches under real sea-surface conditions.

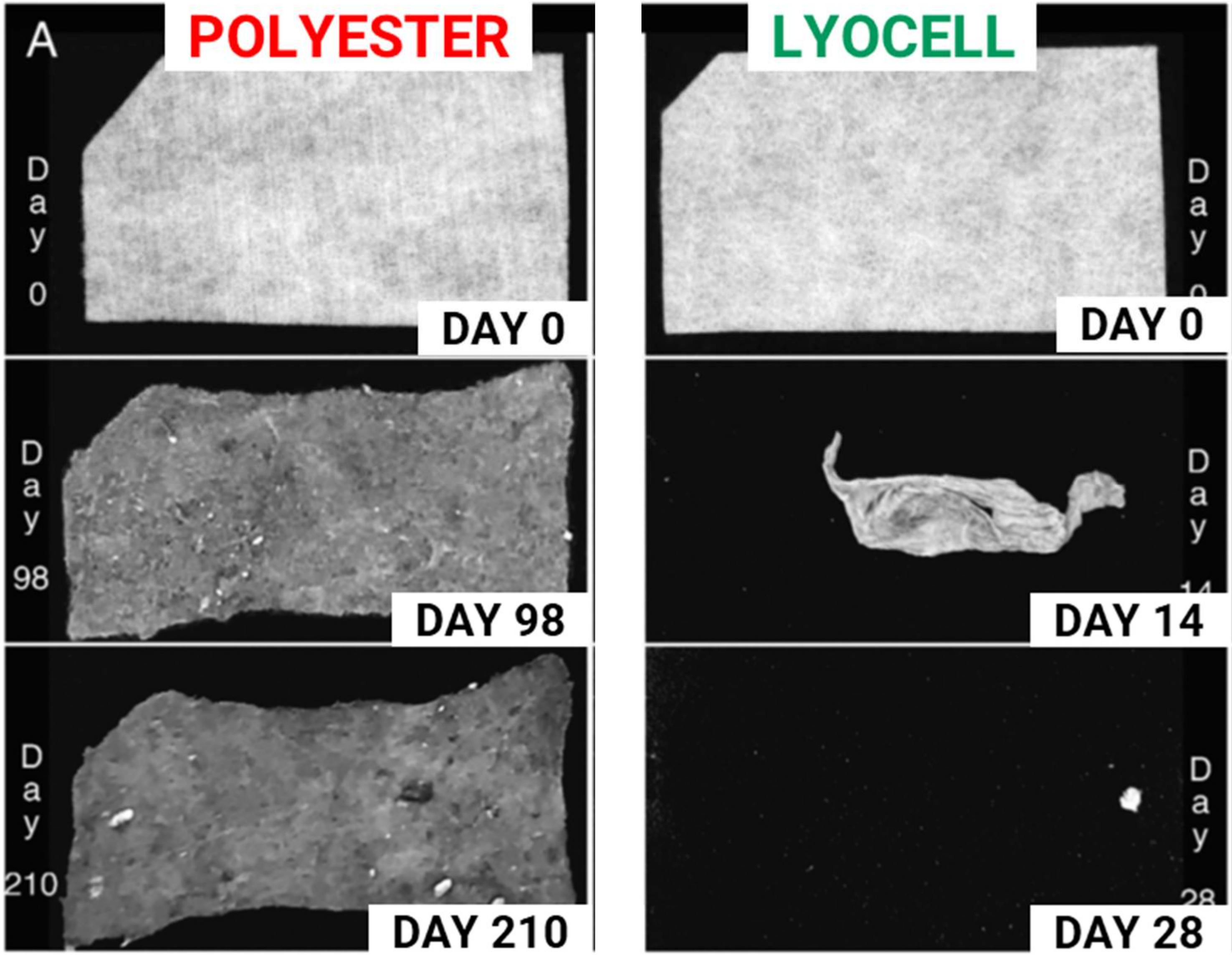

Sarah-Jeanne Royer et al. Science of the Total Environment 791 (2021) 148060

Biodegradation of PET vs CLY in both marine and fresh water

(ASTM D6691, ISO 14851)

UC San Diego | SCRIPPS INSTITUTION OF OCEANOGRAPHY

Sarah-Jeanne Royer et al. Science of the Total Environment 791 (2021) 148060

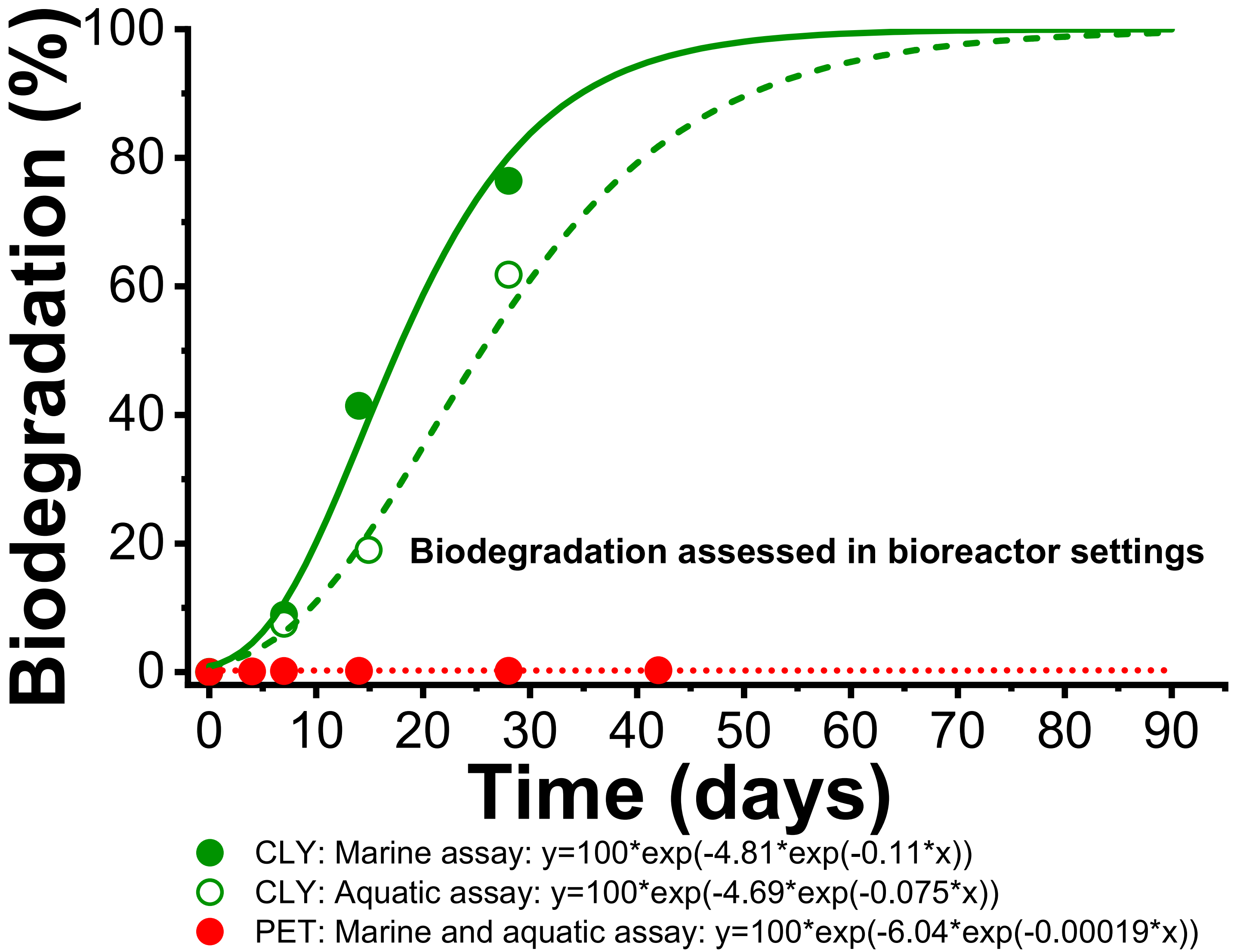

Sarah-Jeanne Royer et al. Science of the Total Environment 791 (2021) 148060

Outline

1. Introduction, history
2. **Pulp as raw material**
3. **Cellulose solvents**
4. **Aspects of cellulose dissolution**
5. **Rheology of cellulose solutions**
6. **Coagulation and regeneration of cellulose**
7. **Filament breaches during spinning**
8. **Types of MMCFs**
9. **Properties of MMCFs**

2

Pulp as raw material

Outline

1. **Introduction**
2. **Applications of dissolving pulps**
3. **Processes to manufacture dissolving pulps**
4. **Controlled DP degradation**
5. Advanced Characterization

What is a Dissolving Pulp?

- Pulp with high cellulose content (>93%)
- with **very low content** of **non-carbohydrate compounds** such as ash, resins, others
- with **defined average molecular weight** and molecular weight distribution
- **highly reactive pulp** enabling rapid and uniform reactions

Standard Specification

	VISCOSE	ACETATE	ETHERS
Intrinsic Viscosity (ml/g)	450	600 - 900	600 - 2000
Hemicellulose (%)	3 - 5	1 - 2	4 - 6
Ash (%)	< 0.1	< 0.05	< 0.2
Si (ppm)	< 20	< 10	< 20
Brightness (%ISO)	89 - 92	> 92	> 85

Molar Mass Distribution

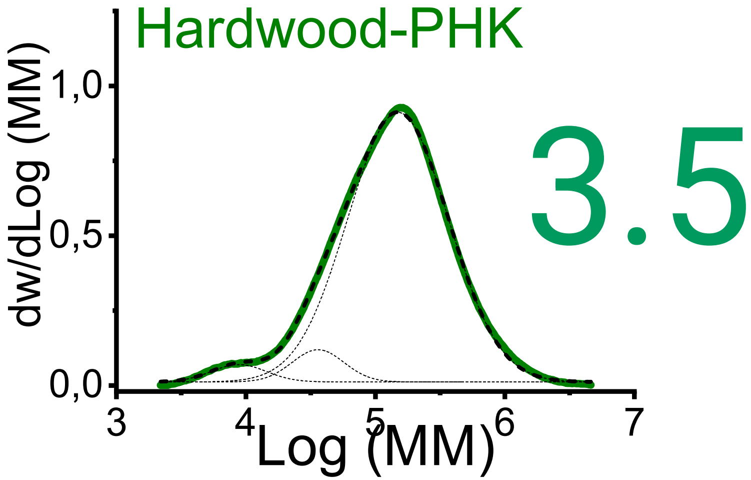

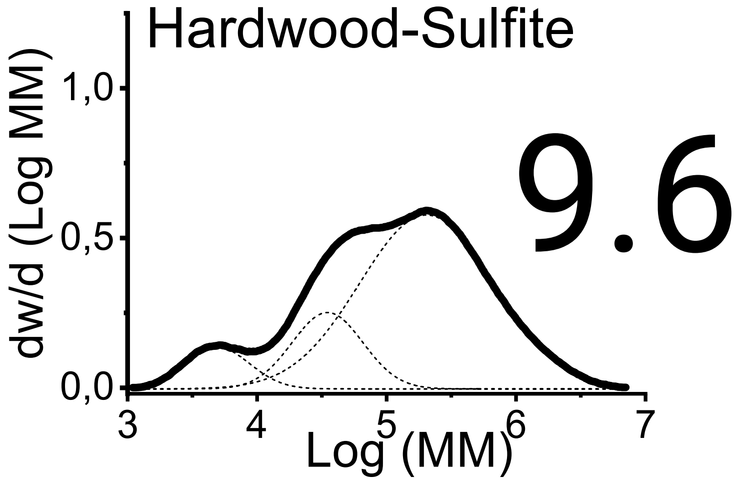

PDI

Poly-Dispersity Index

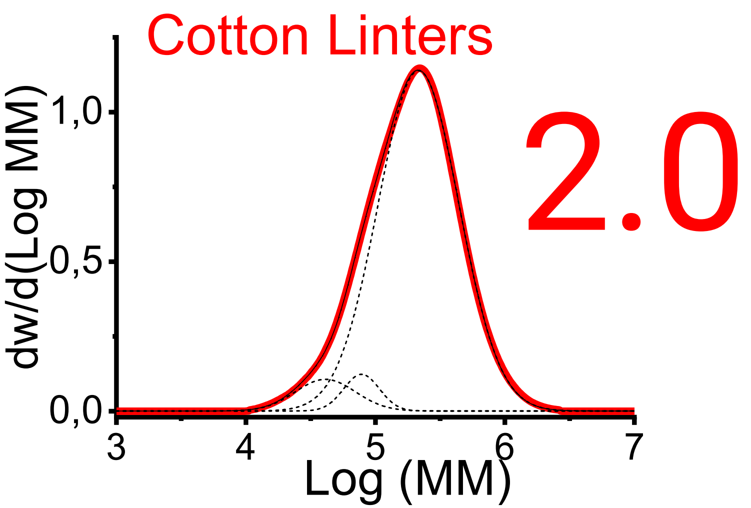

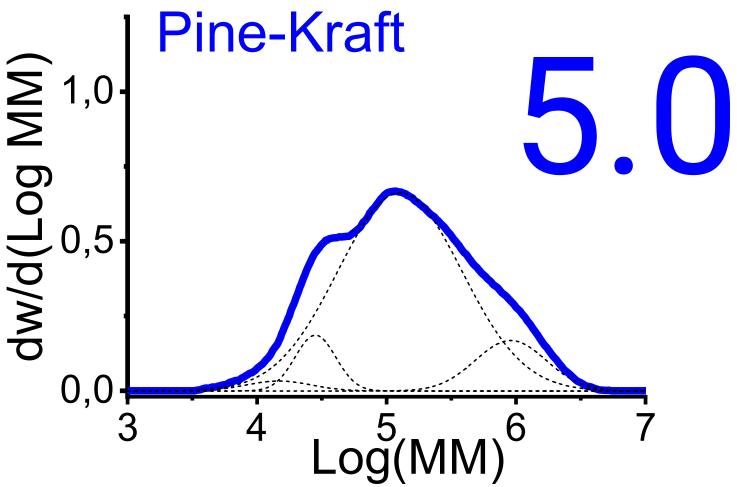

H. Sixta et al., *GPC measurements of commercial DPs*

Dissolving Pulp Capacity by Region

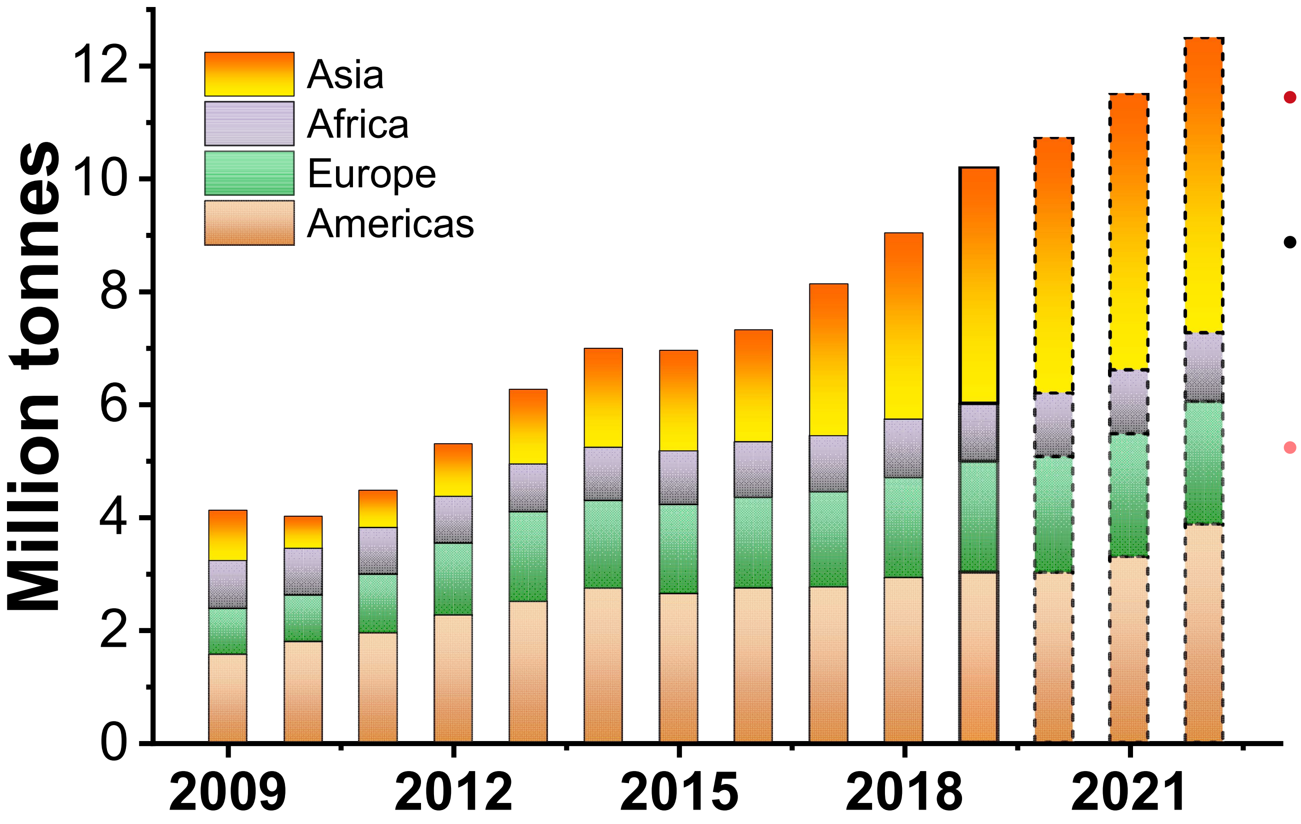

- 2019: 10.2 Mt produced
- Average annual growth during the recent 10 years at 8.4%
- Significant investments, mainly in Asia, have been announced for the coming years

Applications of a Dissolving Pulp?

Textile Fibers
staple
filament
FOURNÉ
Polymertechnik GmbH
Cellulose Acetate
Dry spinning
Filaments
Film
CMC
Cellulose Nitrate
Lacquer
Microcrystalline Cellulose
OxyCellulose
MC

Processes to manufacture dissolving pulps ?

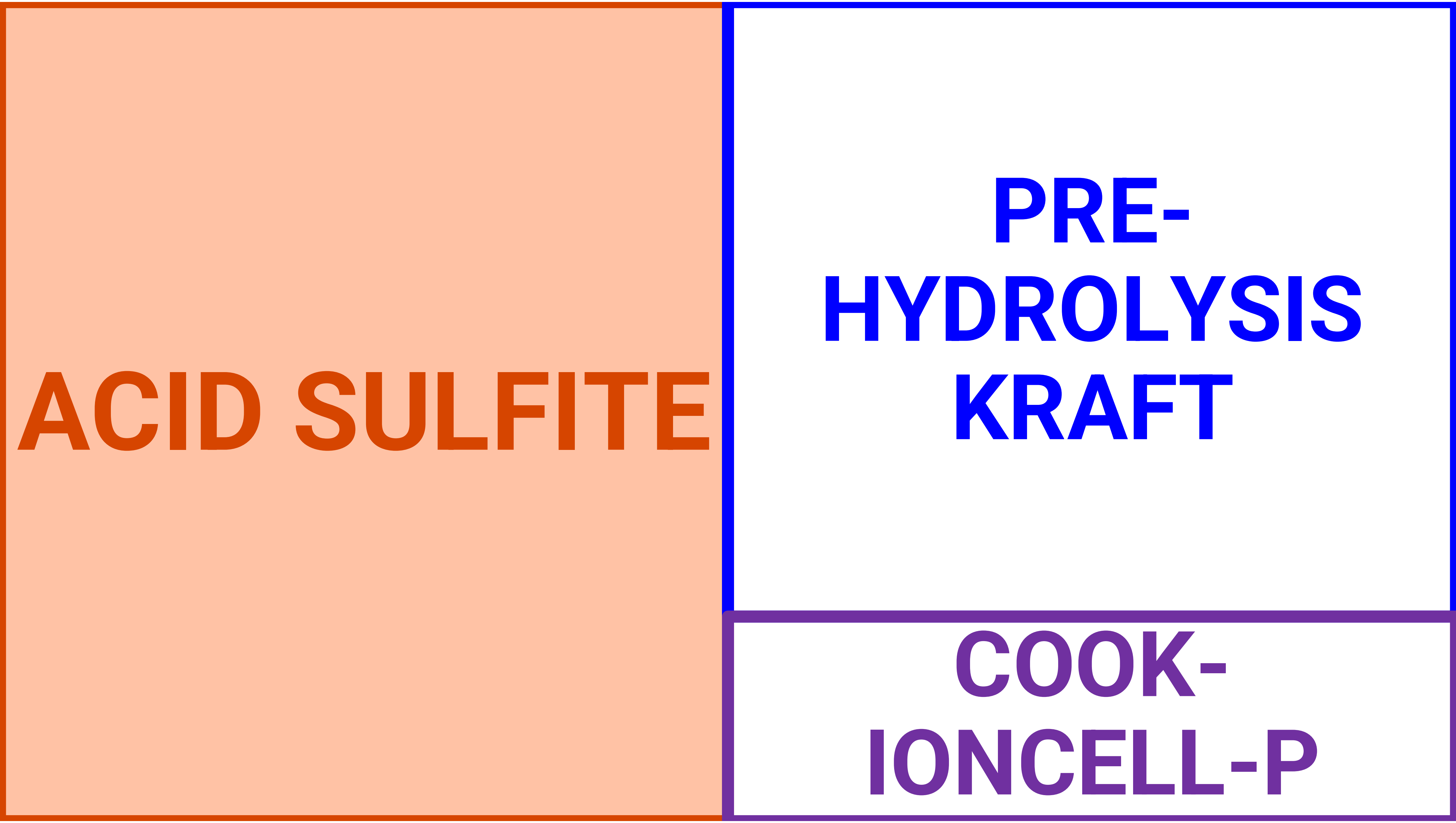
ACID SULFITE
PRE-HYDROLYSIS KRAFT
COOK-IONCELL-P

Purification Methods

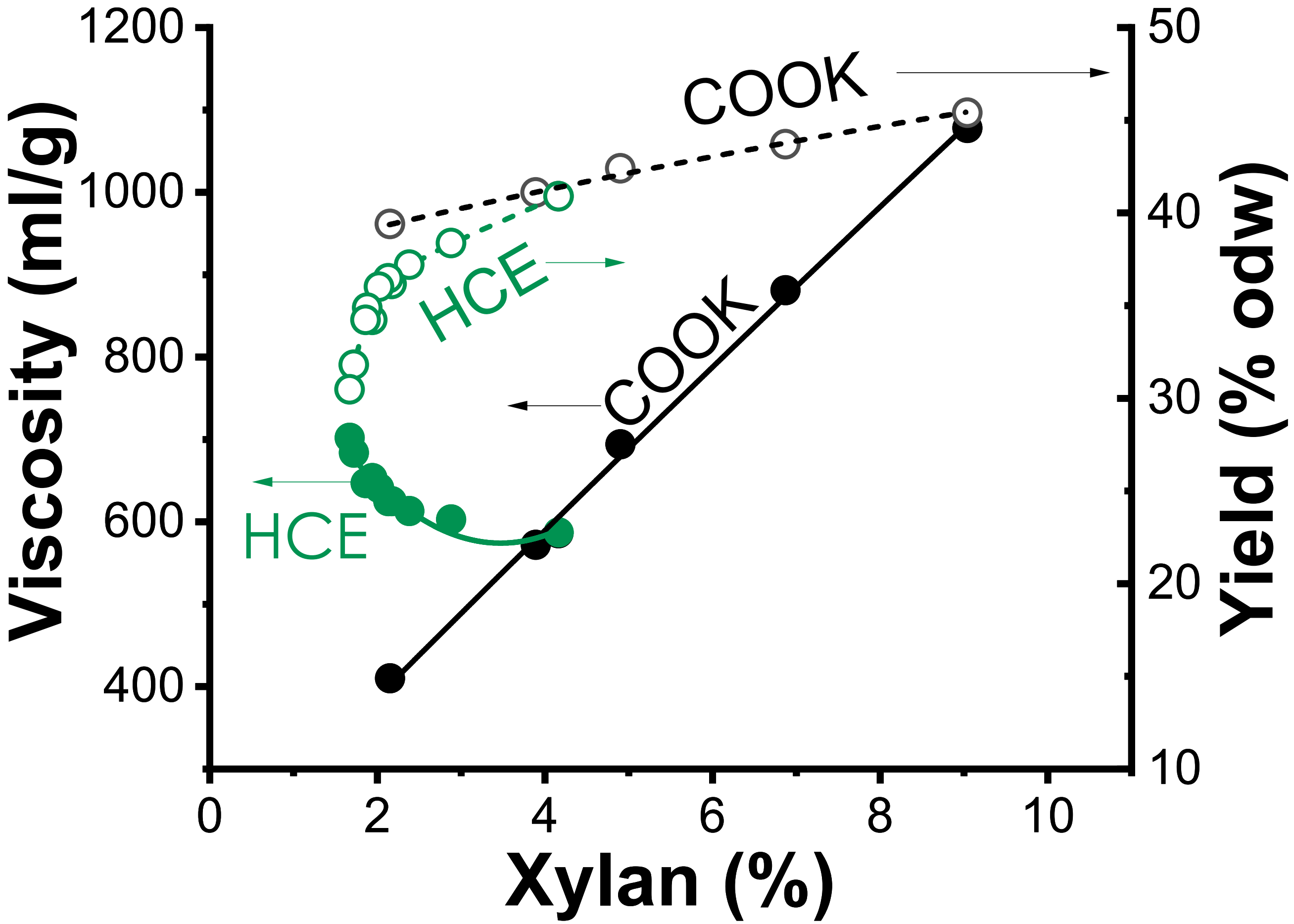

Prolonged Cooking followed by **Hot Caustic Extraction (HCE)**

Beech Acid Sulfite Pulping

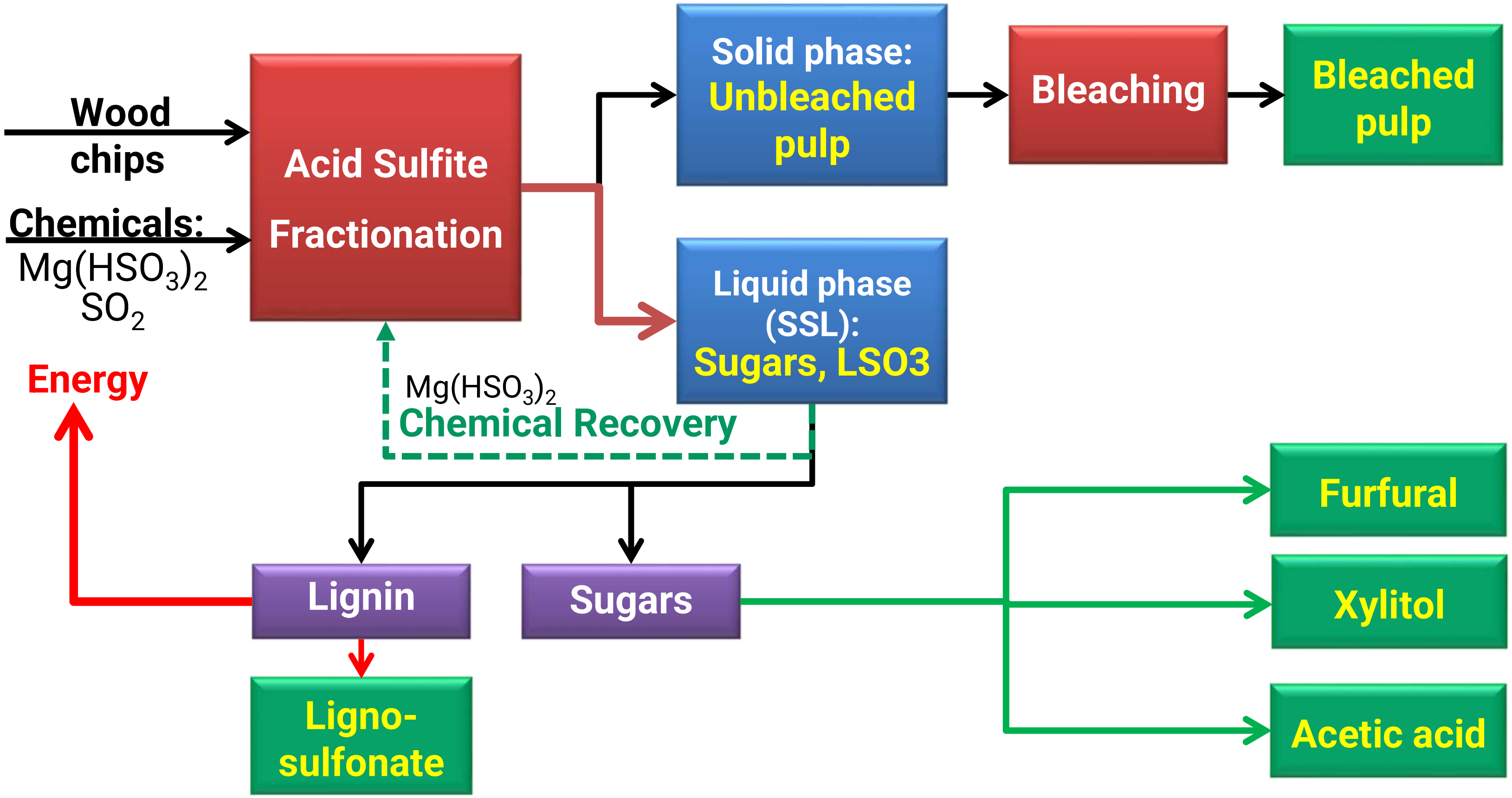

Beech Sulfite Dissolving Pulp Biorefinery

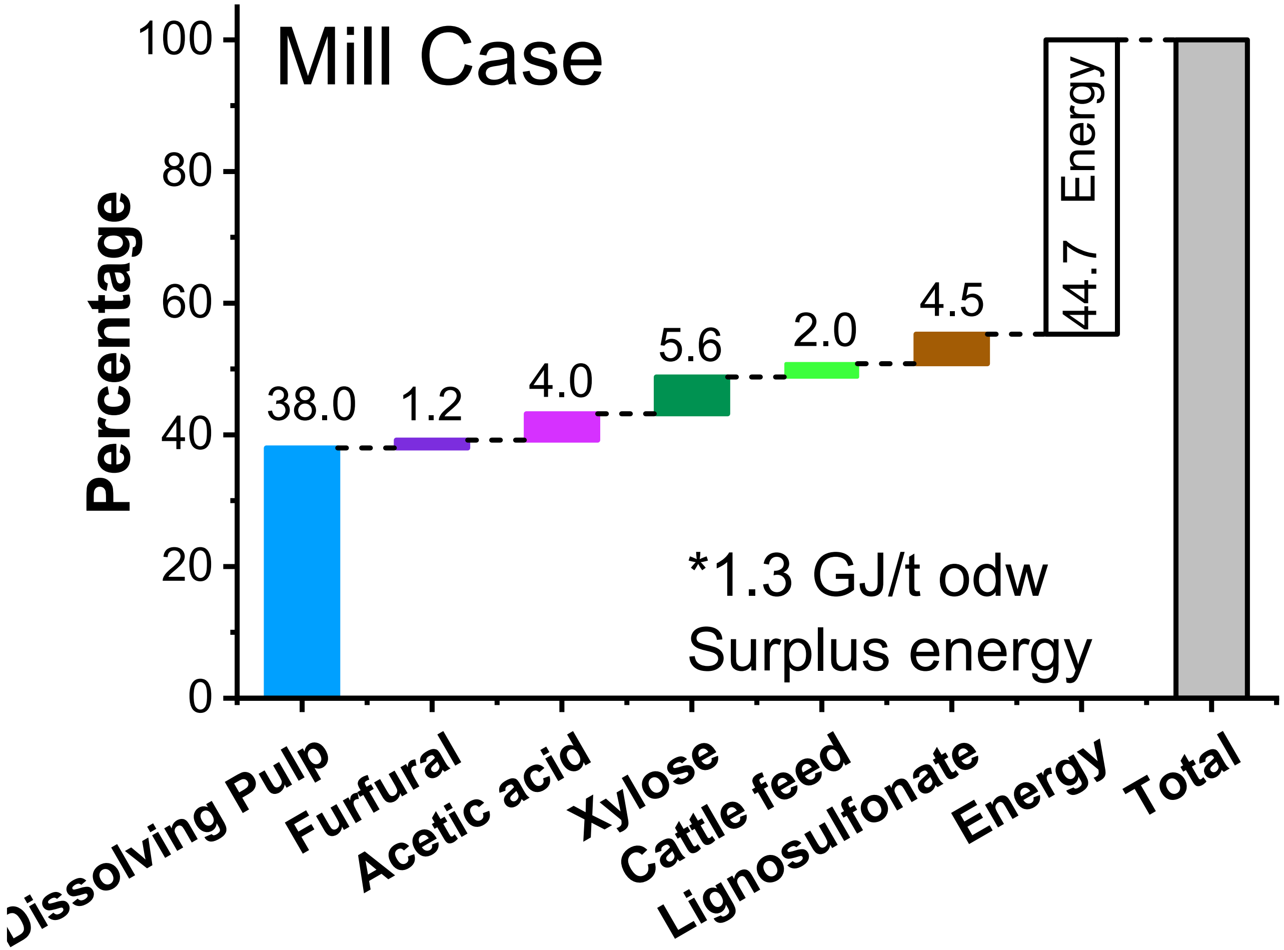

17.3% of the wood utilized as by-product

The future potential of by-product utilisation is estimated to be **20%.**

Spruce Acid Sulfite Biorefinery

Vanillin

from Spent Liquor

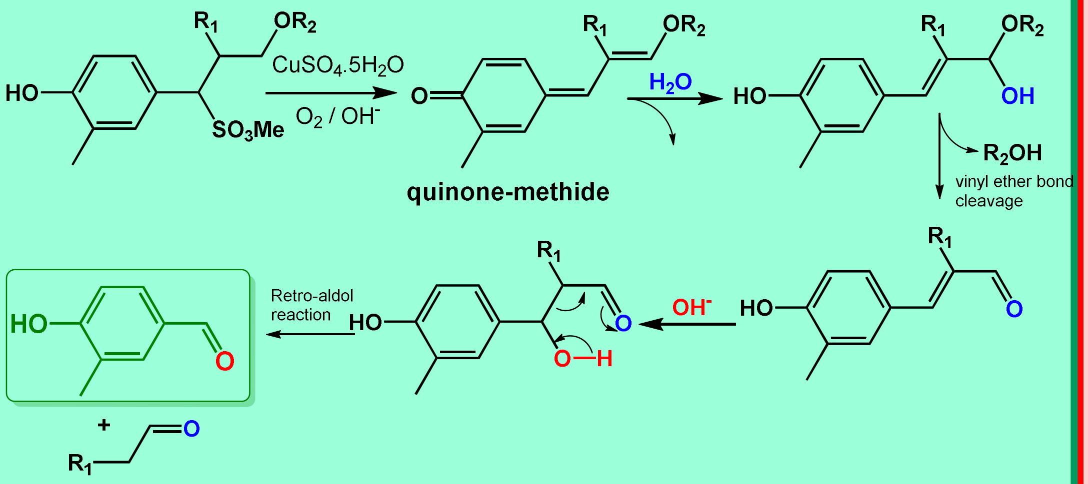

Global production from Lignosulfonate
~ 3000 t/a (15% of global production)

US4,151,207

Cymene

from Digester Relief

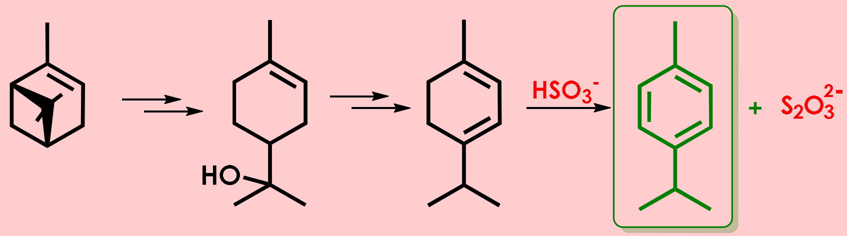

p-Cymene can be added in inks, adhesives, varnishes, pigments, perfumes, pharmaceuticals

ACID SULFITE

PRE-HYDROLYSIS KRAFT

COOK IONCELL-P

Prehydrolysis Kraft (PHK)

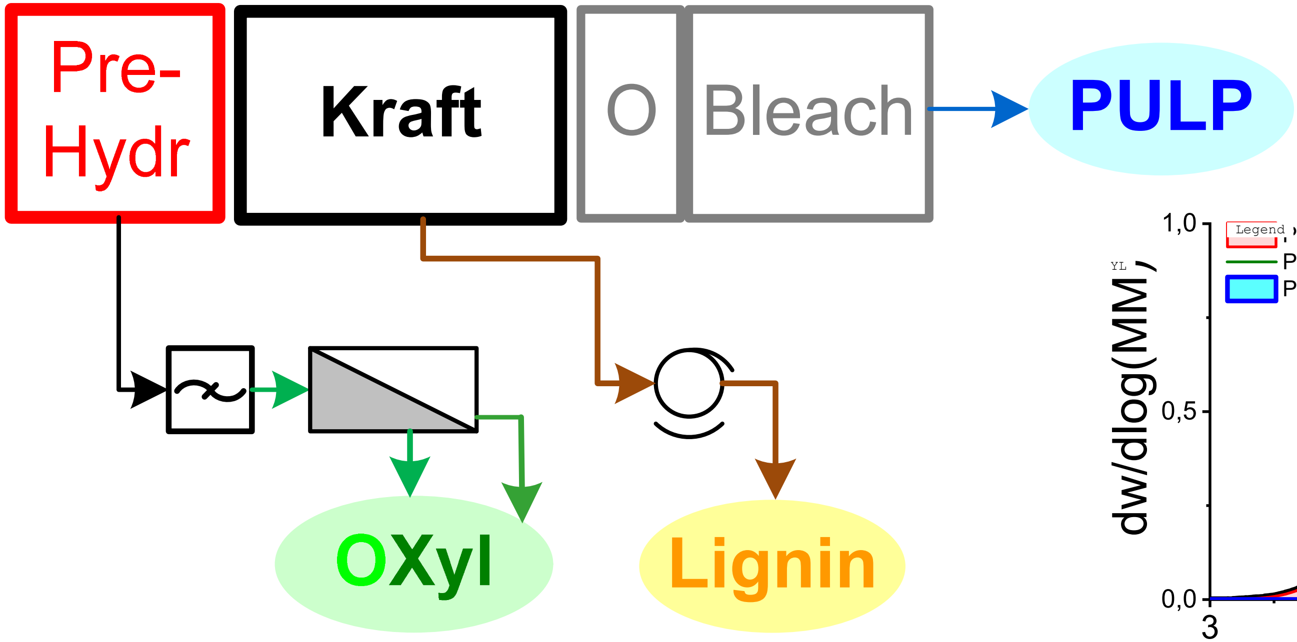

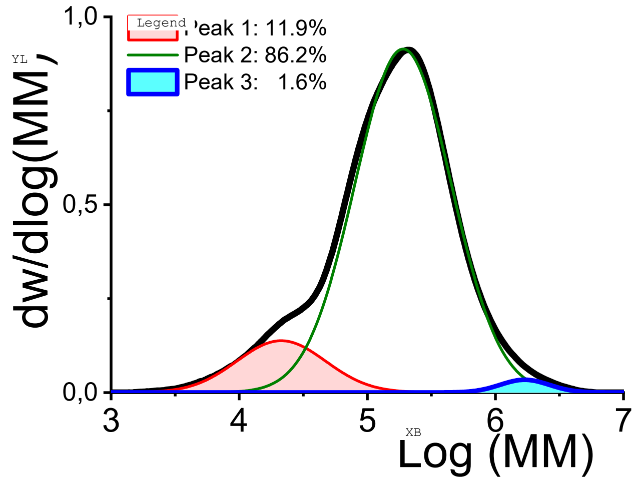

Prehydrolysis Intensity

$$P = \int_{t_0}^{t} \frac{k_{H(T)}}{k_{373K}} \cdot dt = \int_{t_0}^{t} Exp\left(40.48 - \frac{15106}{T}\right) \cdot dt$$

Purification through Prehydrolysis

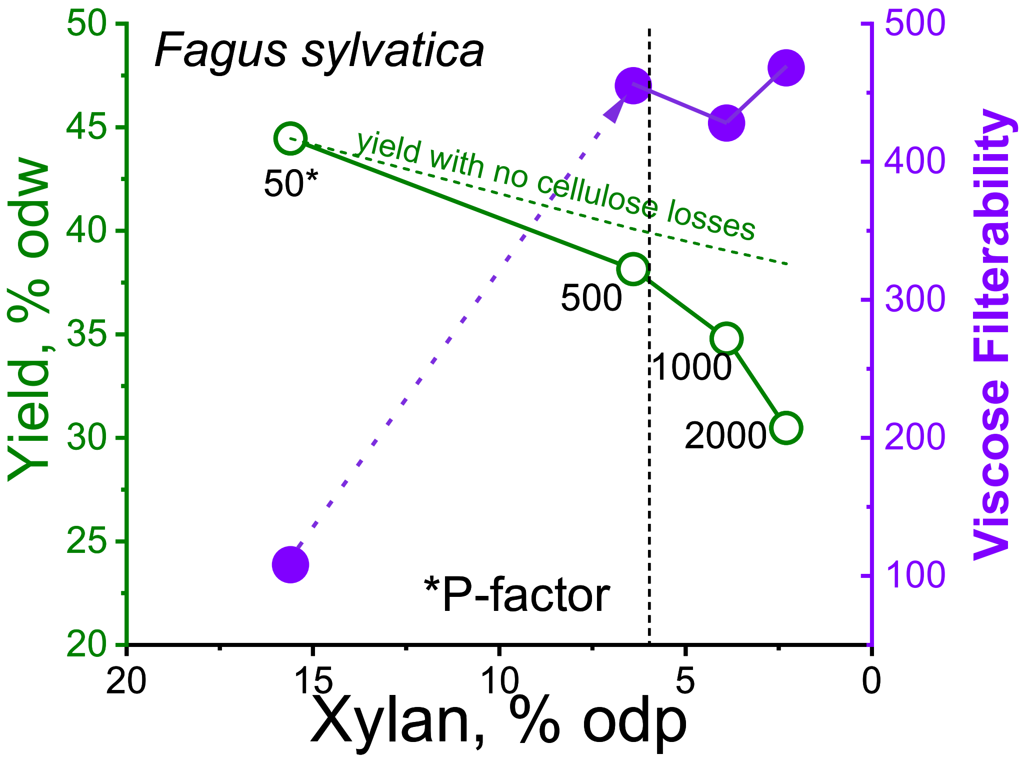

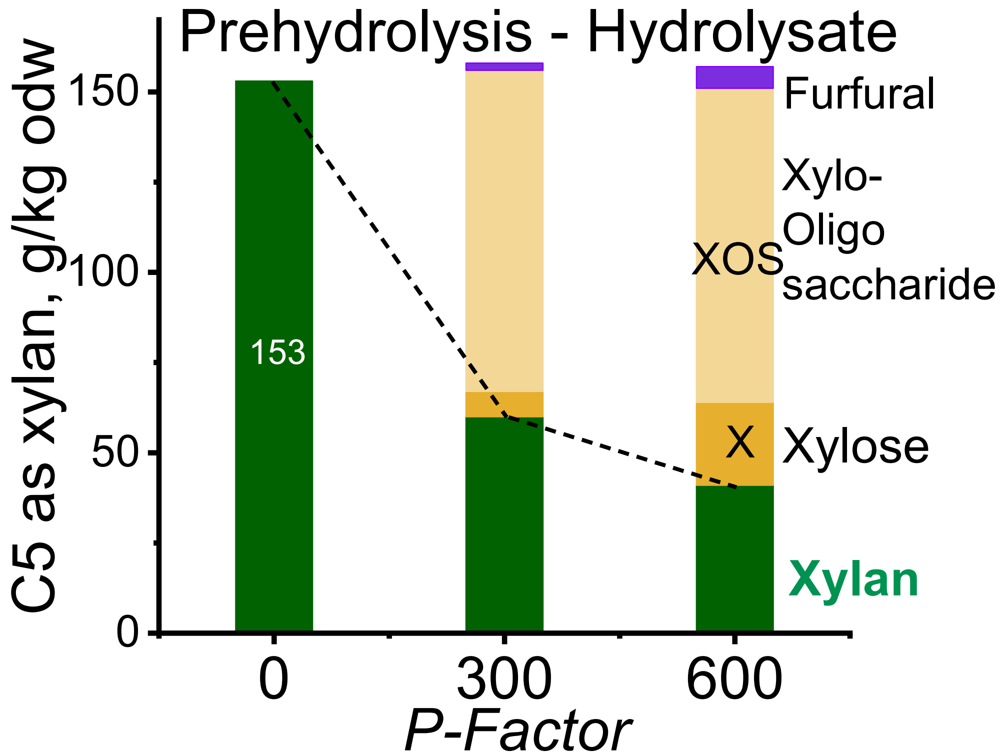

H. Sixta, CDL, unpublished, 2002

Reinforced Purification by PH-CCE

Prehydrolysis and **Cold Caustic Extraction**

Highest-purity Dissolving Pulp

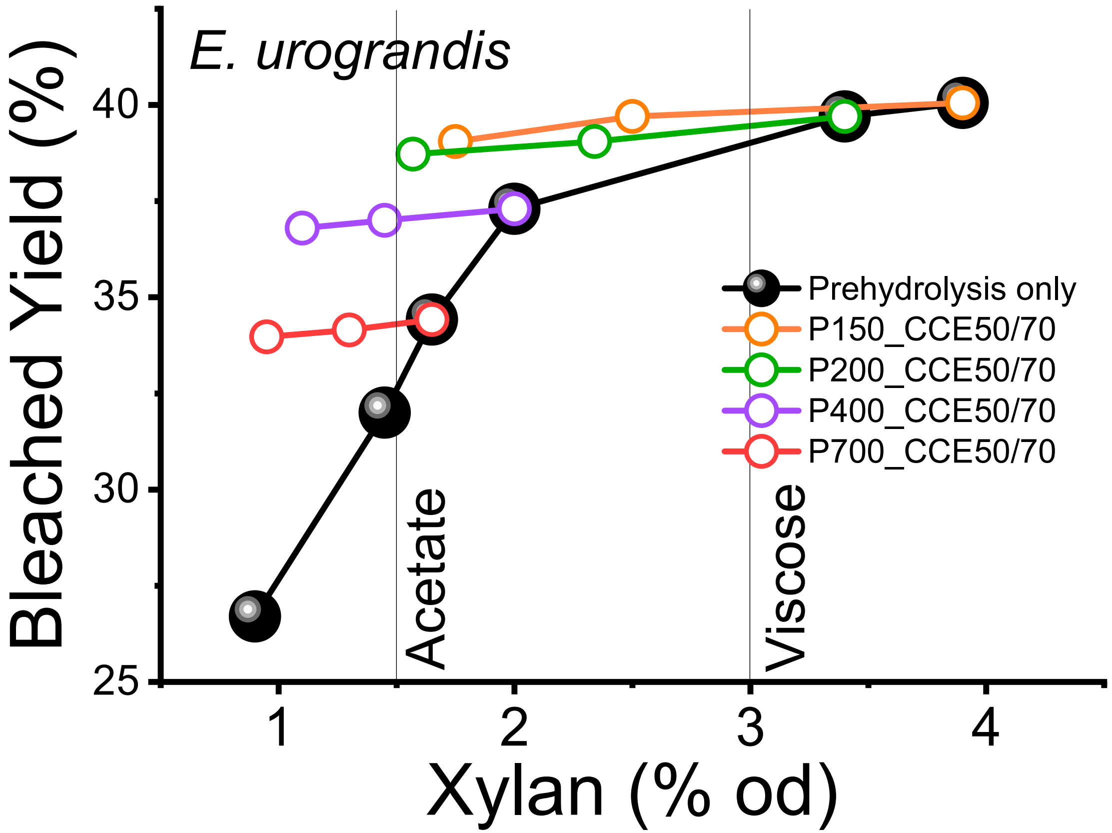

Xylan

as side products

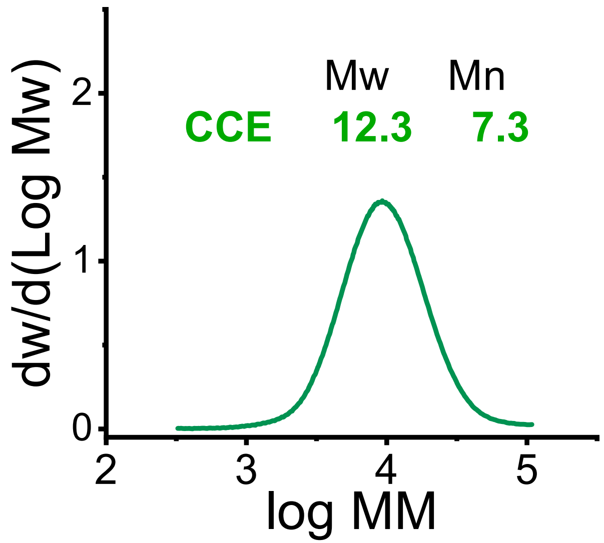

Xylan recovered from CCE filtrate: 3-4% odw

Unpublished results (2000)

Biorefineries

Birch-PHK

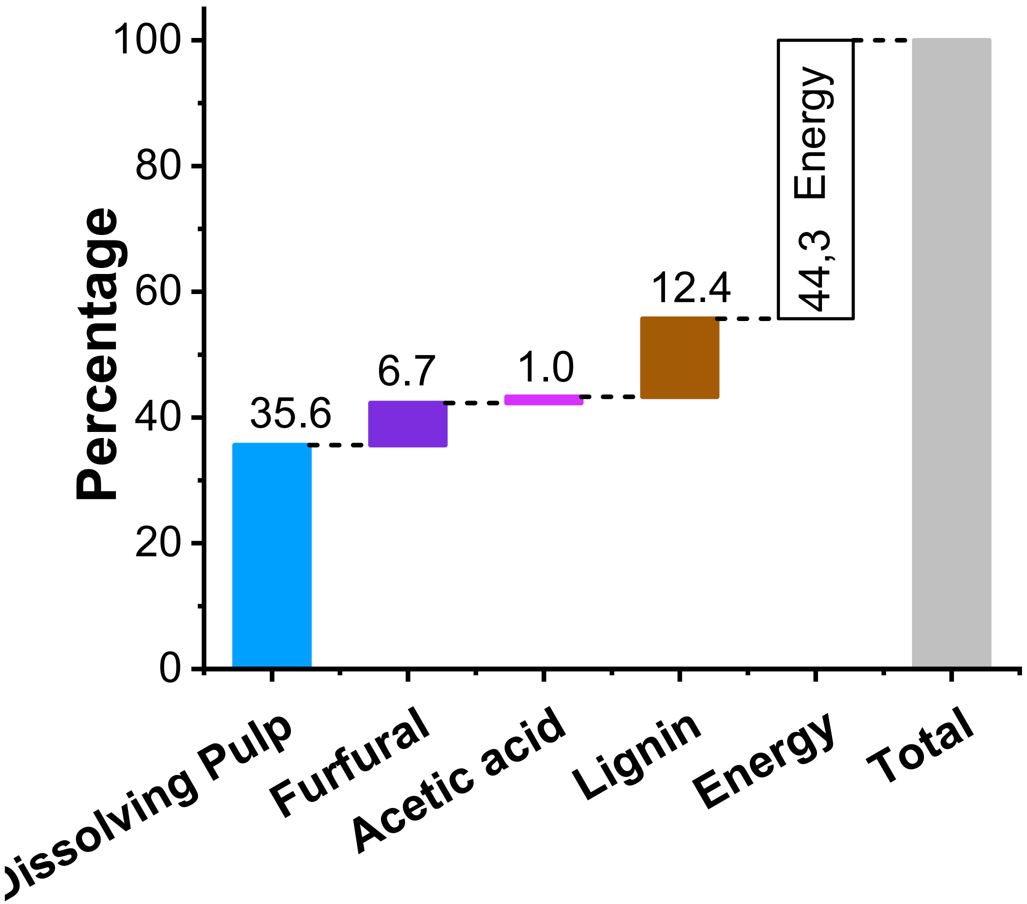

Birch-PHK-CCE

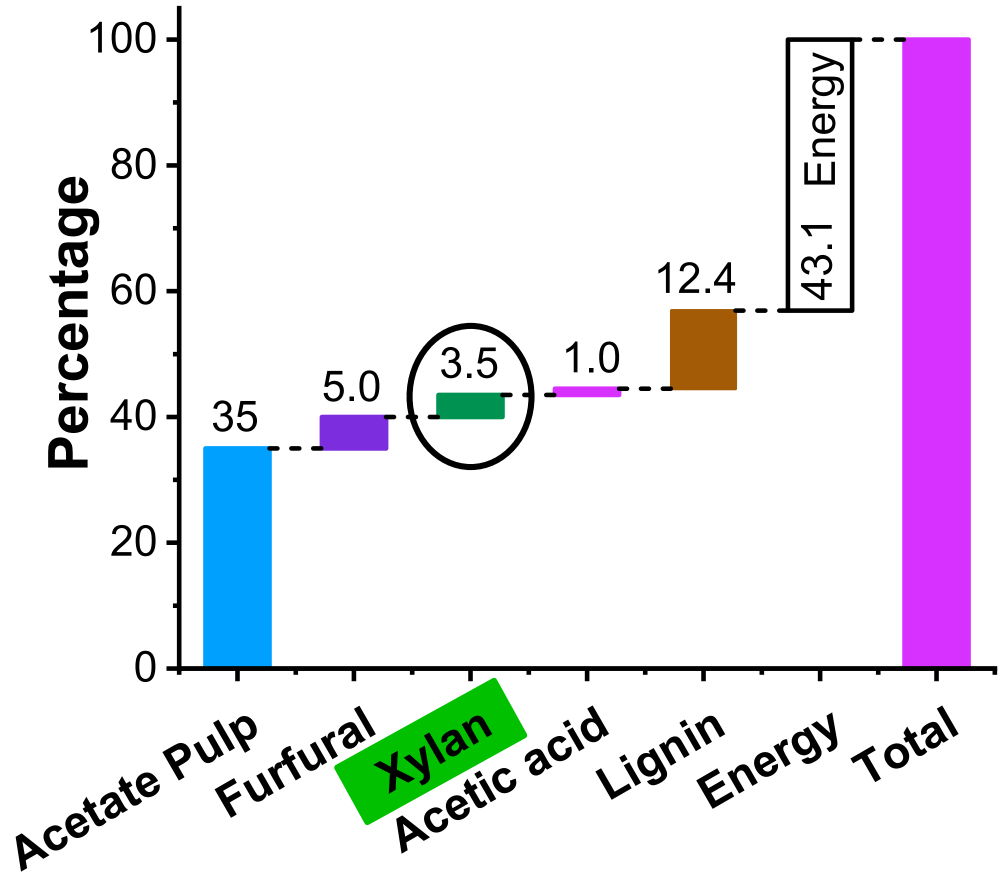

ACID SULFITE

PRE-
HYDROLYSIS
KRAFT

COOK
IONCELL-P

Kamlet-Taft

Empirical solubility parameters to identify solvents for the dissolution of Cellulose and Hemicellulose

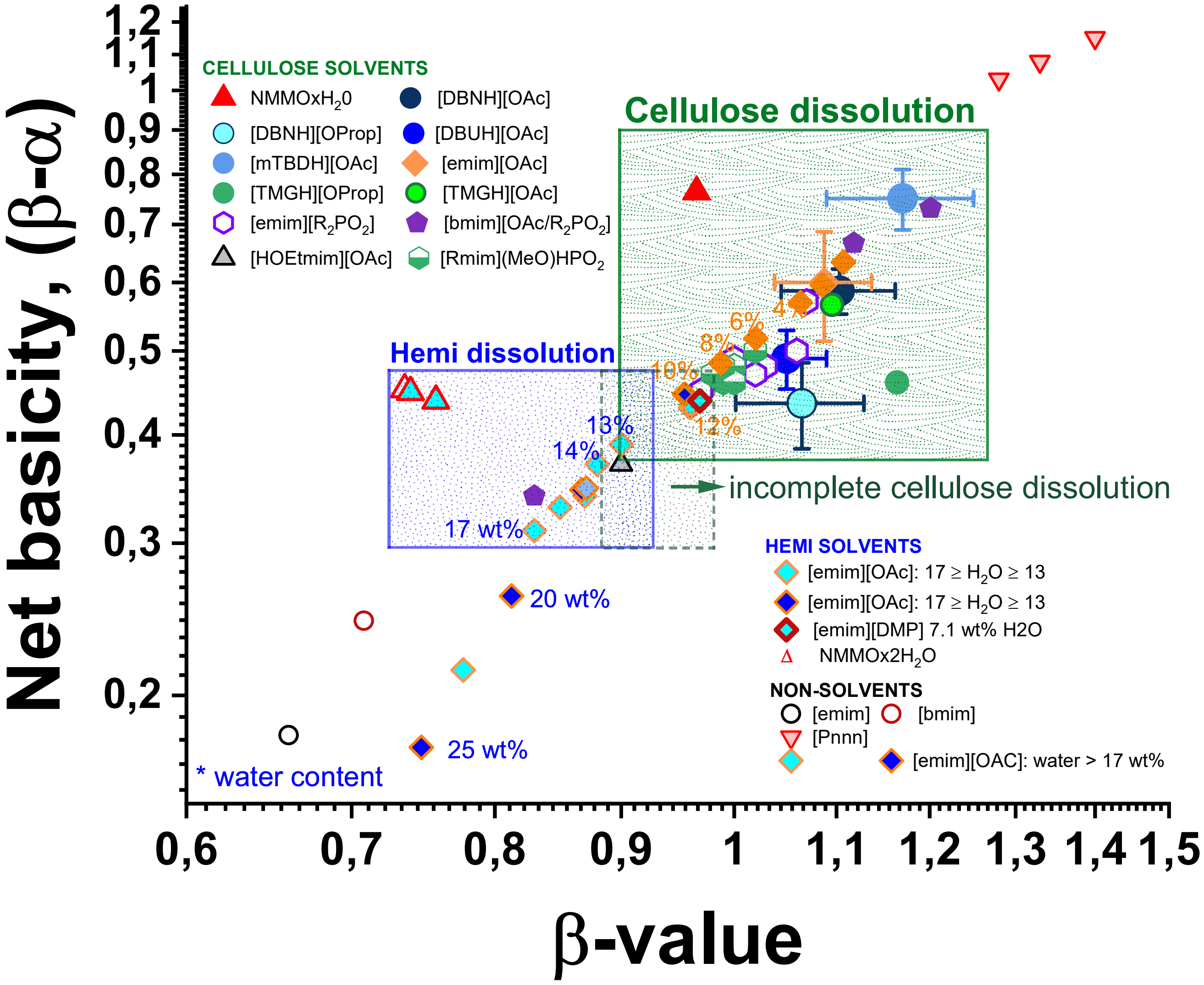

M.J. Kamlet and R.W. Taft: JACS, 98:2, 377-383 (1976)
R.W. Taft and M.J. Kamlet: JACS, 98:10, 2886-2894 (1976)

Ioncell-P Process

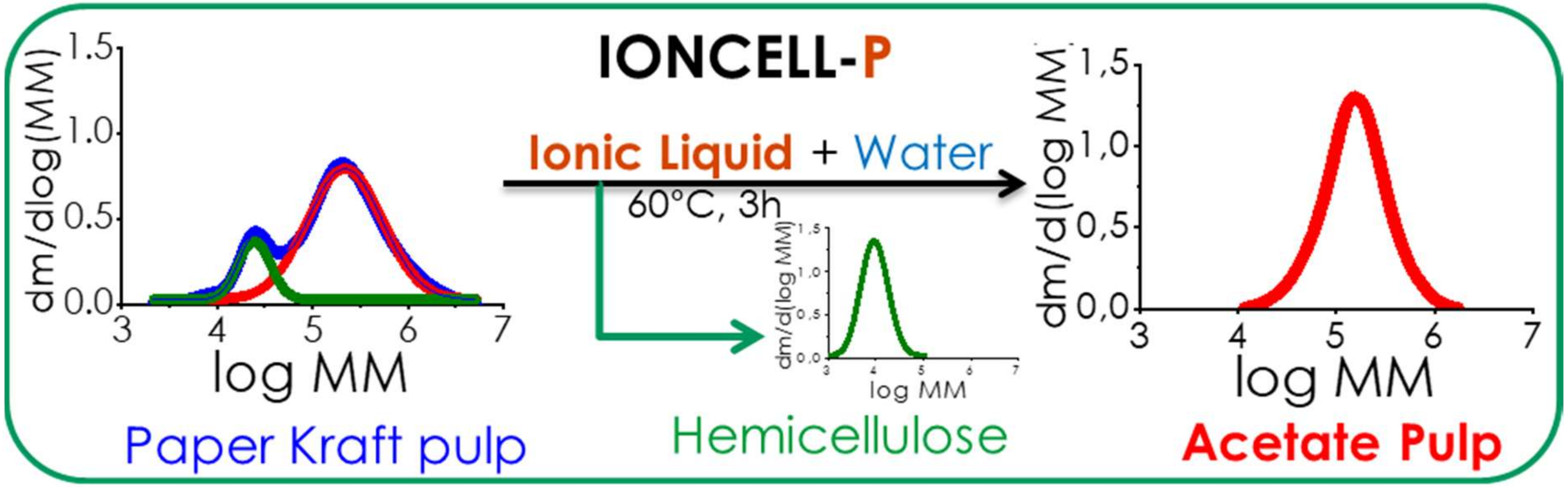

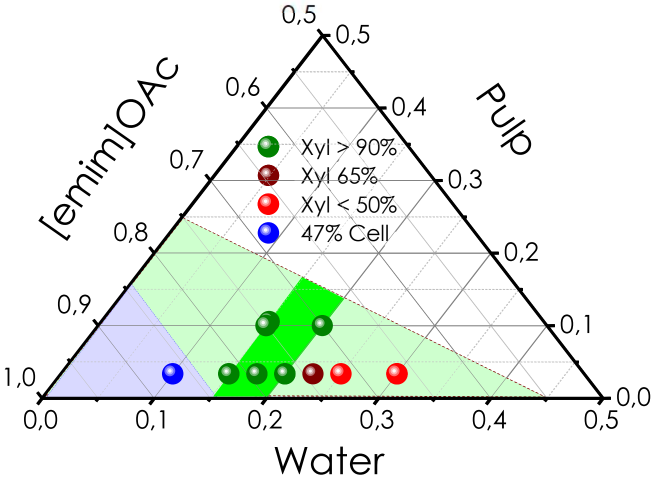

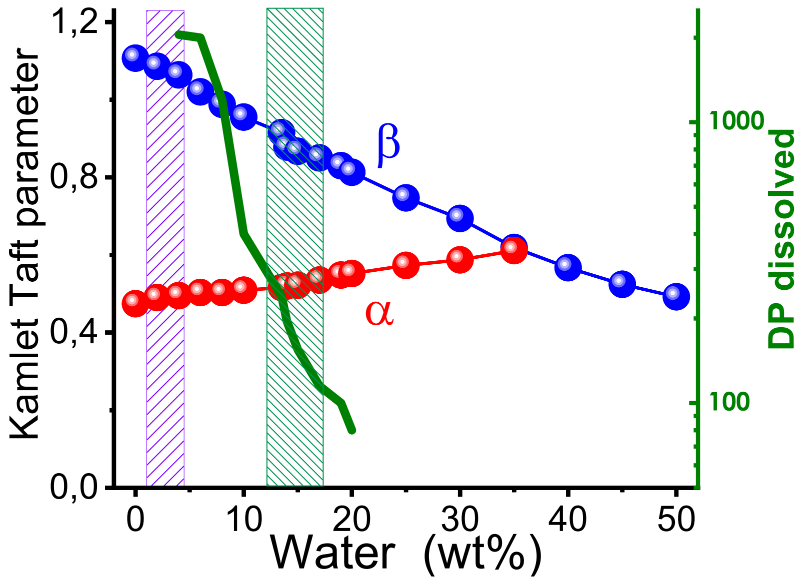

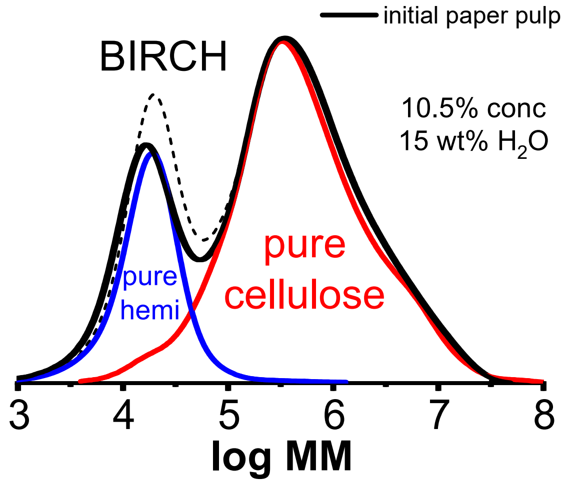

Sixta, H. et al. **WO 2013171364 A1 20131121**
Froschauer C. et al. *Biomacromolecules* **2013**, 14,1741-1750

Ioncell-P treated paper GVL pulp

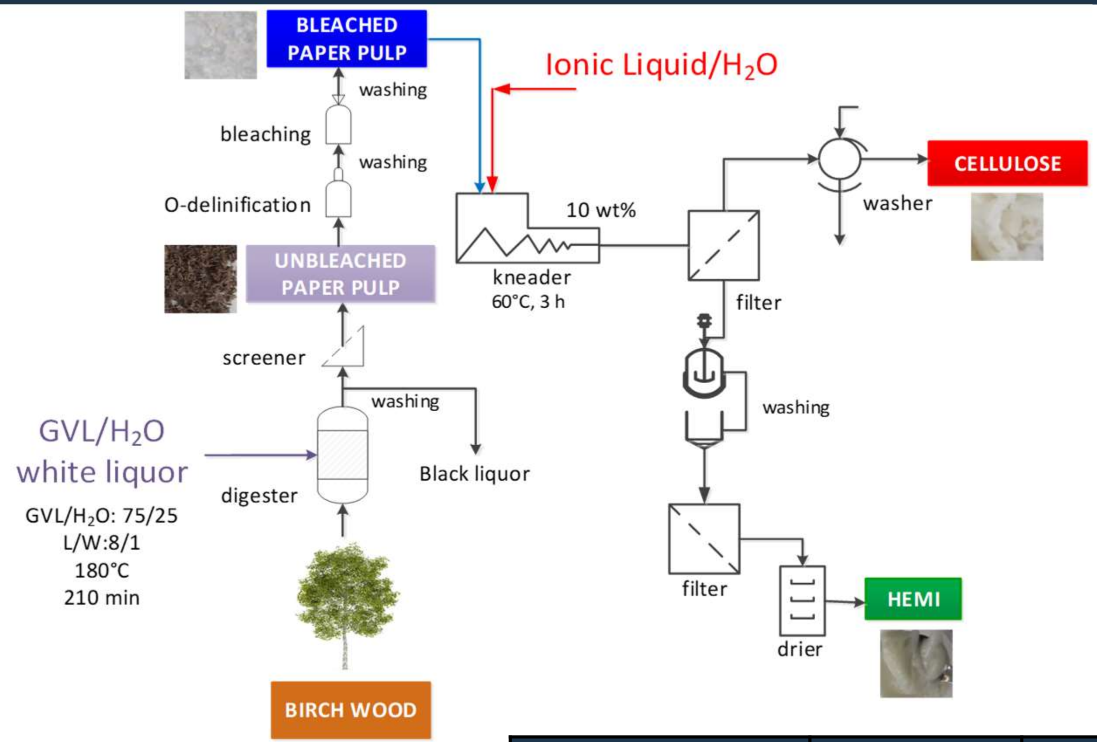

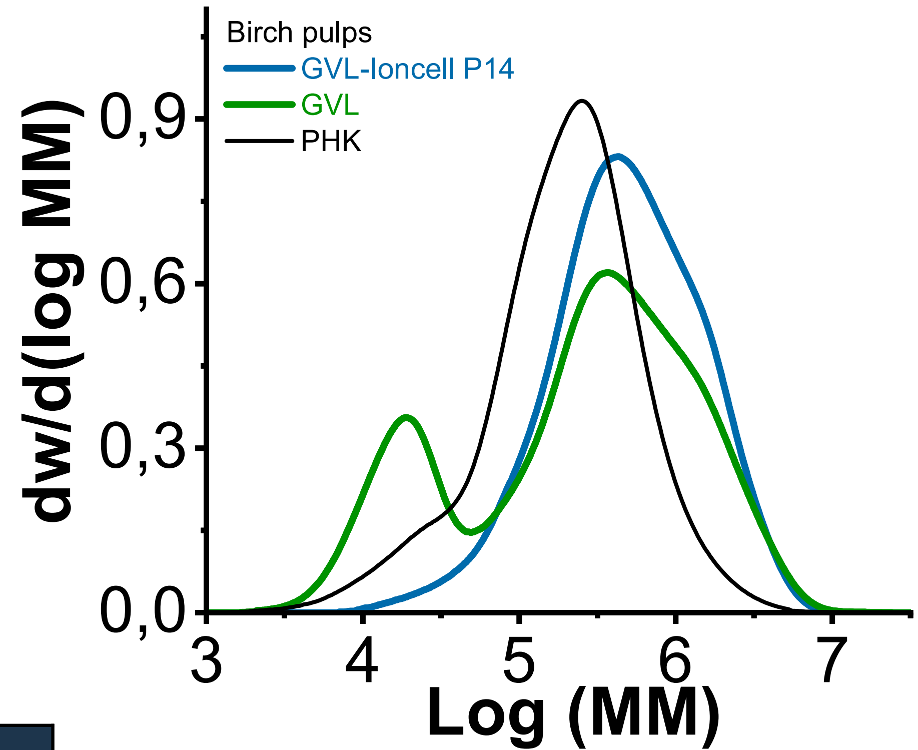

PULPS	Viscosity (mL/g)	Xylan (%)
GVL	1056	18.7
GVL-IP-15%	1266	2.1
GVL-IP-17%	1258	2.8
Reference PHK	468	6.8

Shokoufeh, S. et al. submitted to Carbohydrate Polymer (2022)

Production of a high-viscosity, high-purity pulp in two sequential steps using two green, recyclable solvents as the only chemical input.

Controlled Deploymerization?

Controlled Depolymerization of Dissolving Pulps

1. Acid hydrolytic chain cleavage

2. Endoglucanase treatment

3. Ozone induced chain scission

4. Oxidative alkaline degradation (aging)

5. Electron beam irradiation

Definitions

1. Adjustment of the desired DP
2. Improvement of accessibility
3. Control of the molecular mass fraction (?)

Definition:

$\frac{DP_0}{DP_j} - 1$**:** Chain Scission per chain

$\frac{10^4}{P_j} - \frac{10^4}{P_0}$: Chain scission per AHG.

Endoglucanase treatment

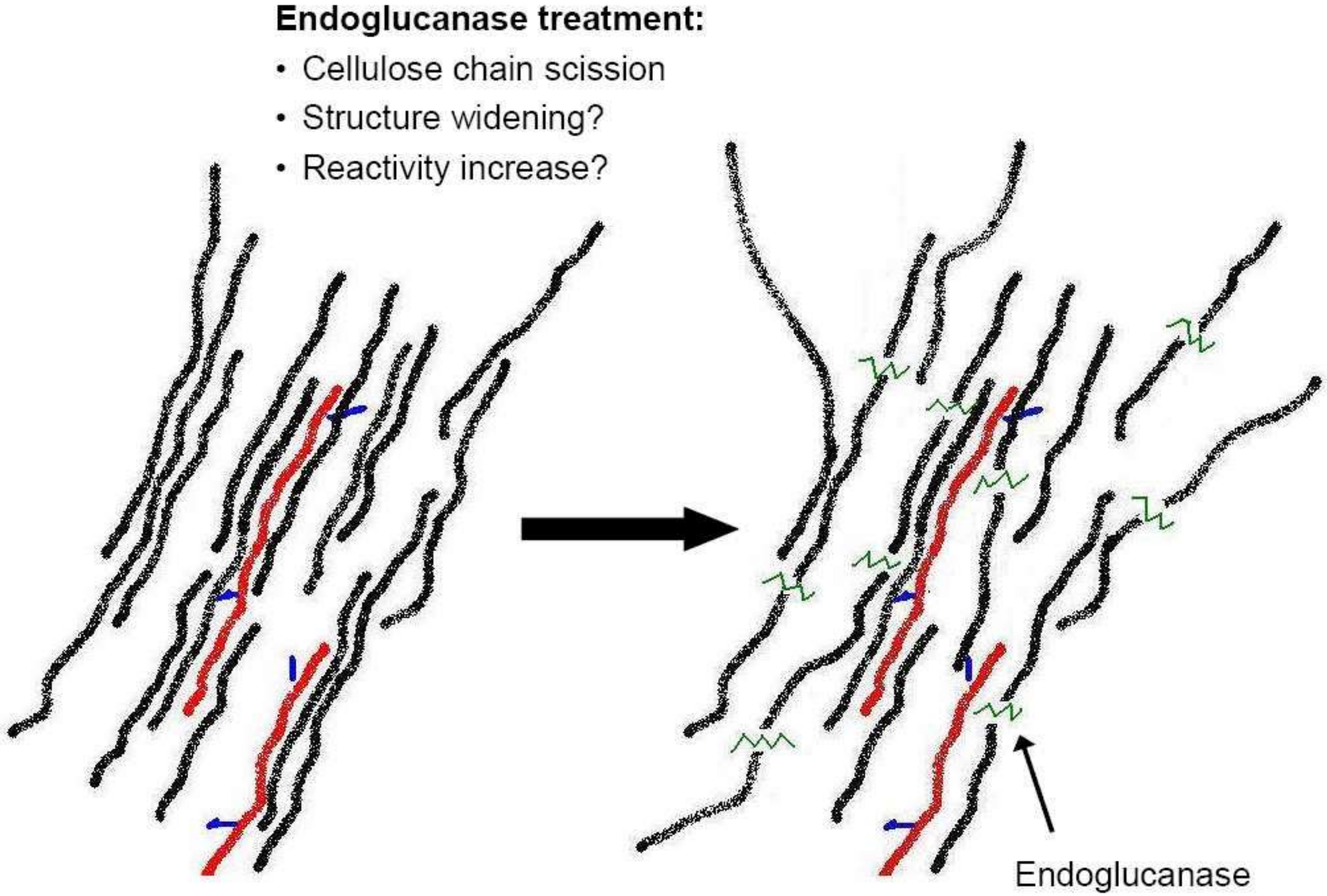

Verena Gehmayr: PhD Thesis (2012), TUG

Endoglucanase treatment

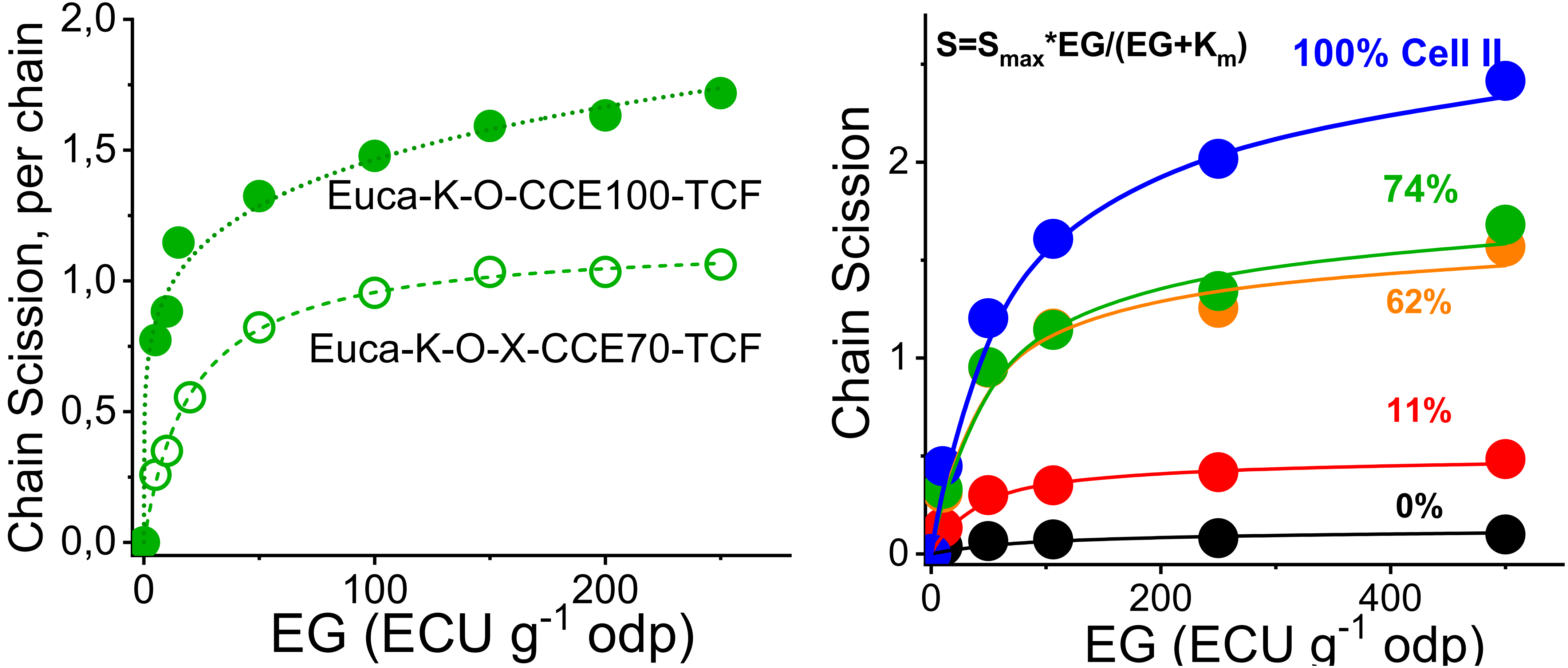

Verena Gehmayr: PhD Thesis (2012), TUG

Effect of Endoglucanase treatment

- Cellulose II structure more accessible; increased unit cell dimensions, & WRV

- EG accessibility is facilitated in the absence of hemicellulose and in the **absence of lignin**.

Verena Gehmayr: PhD Thesis (2012), TUG

Ozone treatment

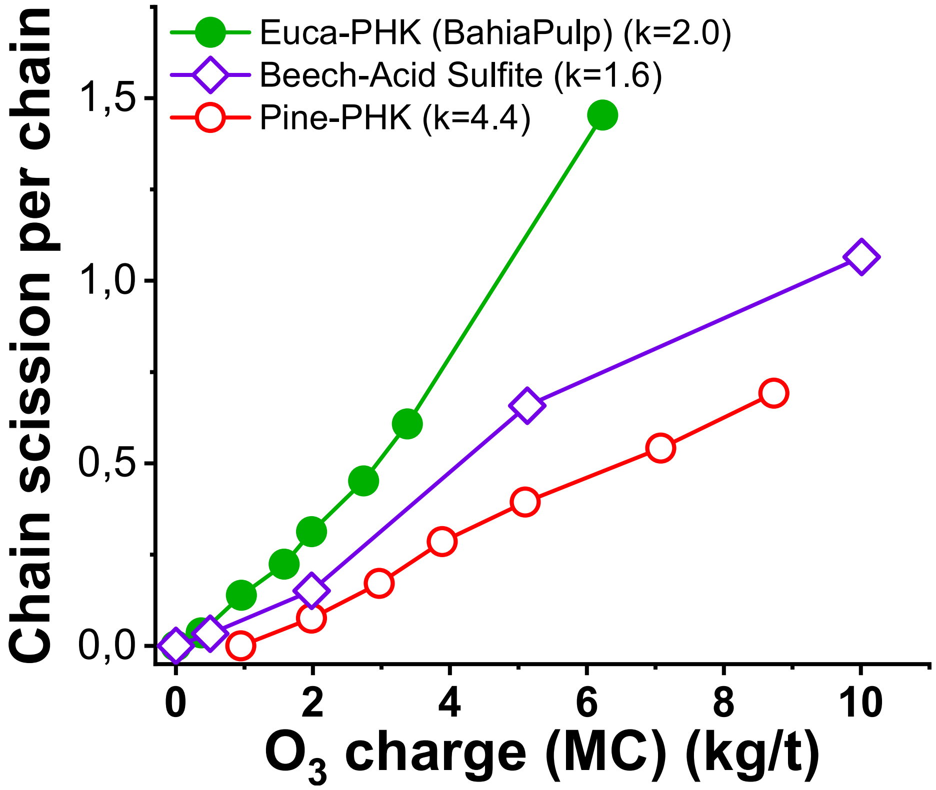

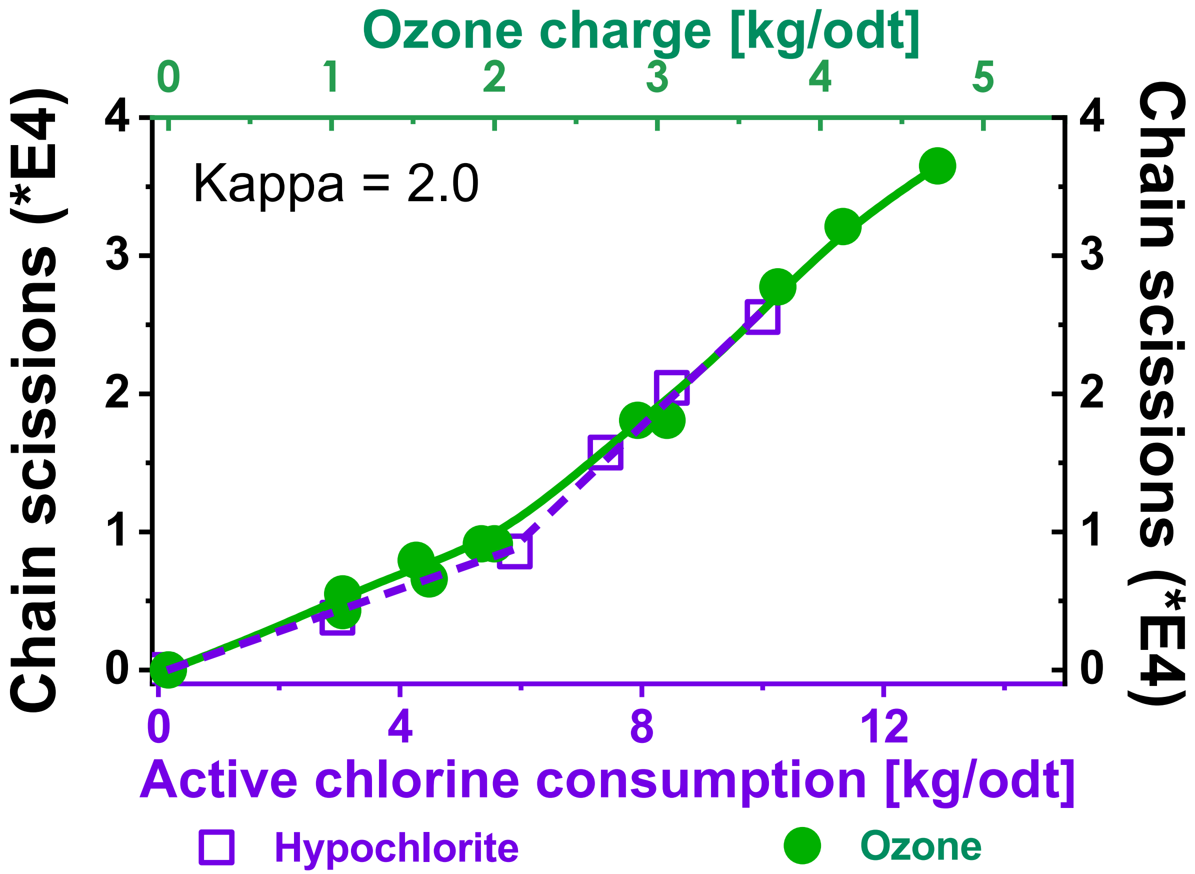

Sixta, H (2006), Handbook of Pulp and Unpublished results

Ozone treatment

- Residual lignin competes for ozone: decreased slope.
- Presence of hemicellulose for the same type of pulp protects cellulose against depolymerization.
- Ozone attack: Shrinking core mechanism
- Morphologie: thin primary cell wall facilitates accessibility

Sixta, H (2006), Handbook of Pulp and Unpublished results

Effect of ozone treatment on MMD

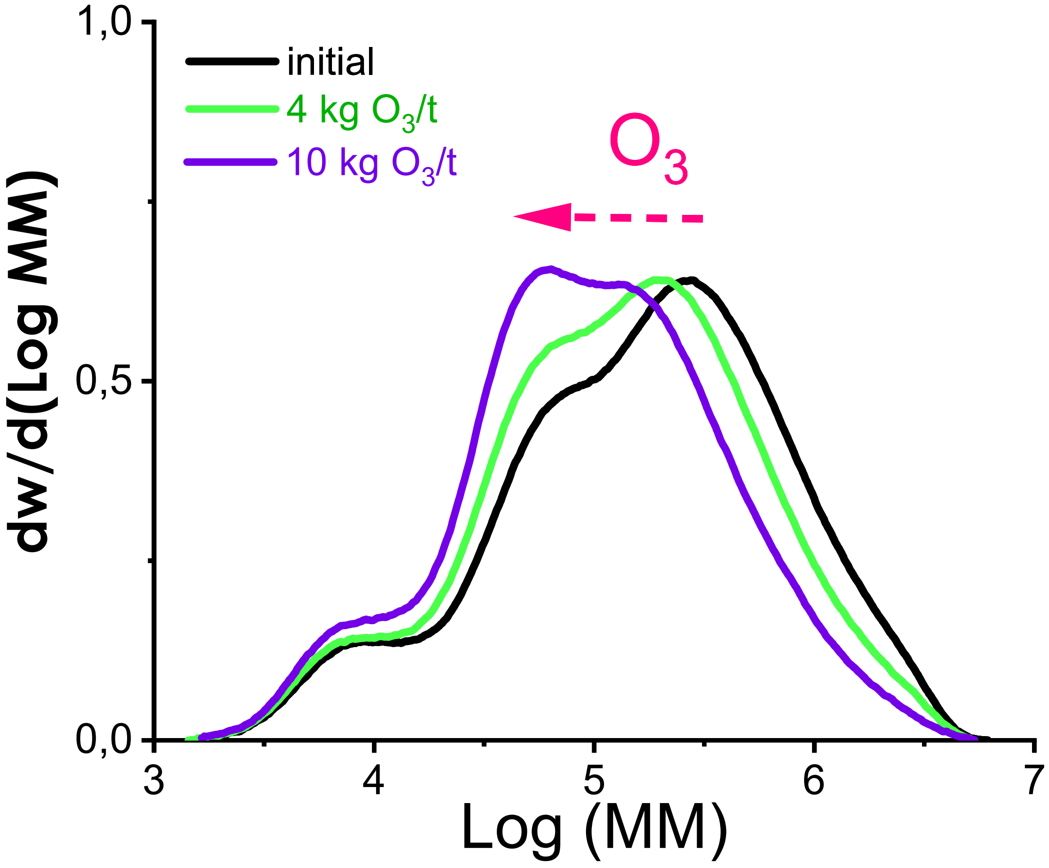

Sixta, H (2006), Unpublished results

Electron beam irradiation

To adjust the DP of pulp and improve accessibility.

Free radical formation leads to the formation of CO and COOH groups.

1 Gray (Gy) = 100 rad

$1\ Gy = J \cdot kg^{-1} = m^2 s^{-2}$ absorbed dosage

$1\ Gy = 6.25 \cdot 10^8 eV kg^{-1}$

G-Factors

Effects of irradiation of cellulose:

Involves the measurement of the changes, *e.g*. molecular weight, molecular weight distribution:

G is defined as the event yield per 100 eV of energy deposited in the material.

G is the irradiation yield: number of chain scissions per 100 eV absorbed radiation energy [mol/J].

$$G = \frac{\frac{CS}{AHG}}{f_1 \cdot dosage\ in\ kGy \cdot f_2}$$

$$f_1 = \frac{molecules}{100\ eV} = \frac{6.023 \cdot 10^{-23}}{1.602 \cdot 10^{-17}} = 1.0364 \cdot 10^{-7}\ mol/J$$

$$f_2 = \frac{10^3 \cdot 162g}{mol \cdot 1000g}$$

$$\boldsymbol{G = \frac{\frac{CS}{AHG} \cdot 10^4}{0.1679 \cdot dosage\ in\ kGy}}$$

Fischer, 1985; Goldberg, 1989

Electron beam irradiation

Accelerator: 10 MeV (bis 200 kW, 20 mA)

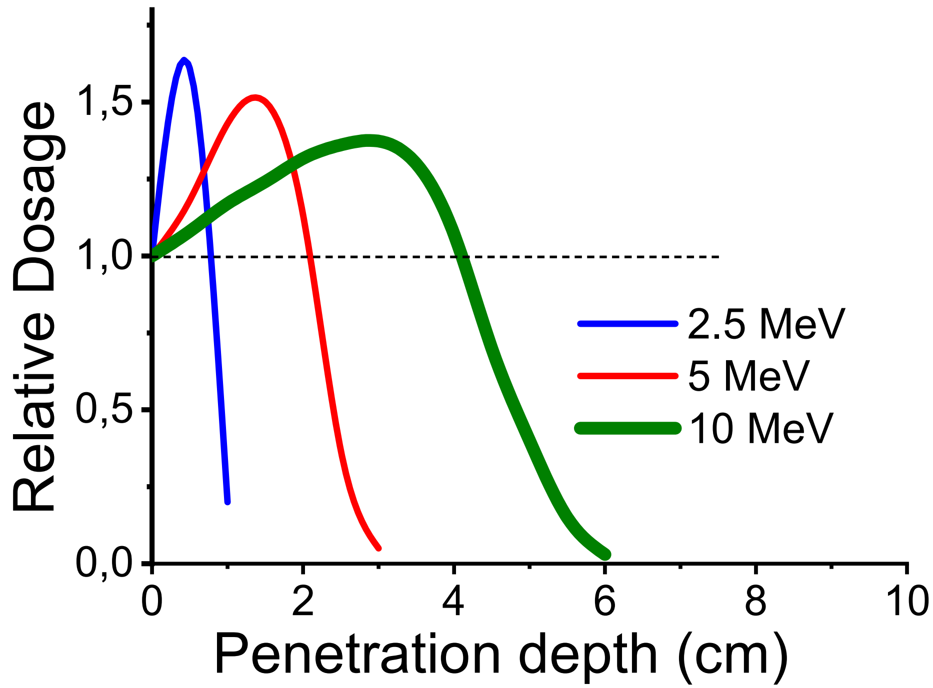

Distribution of the dosage as a function of the penetration depth

Electron beam irradiation

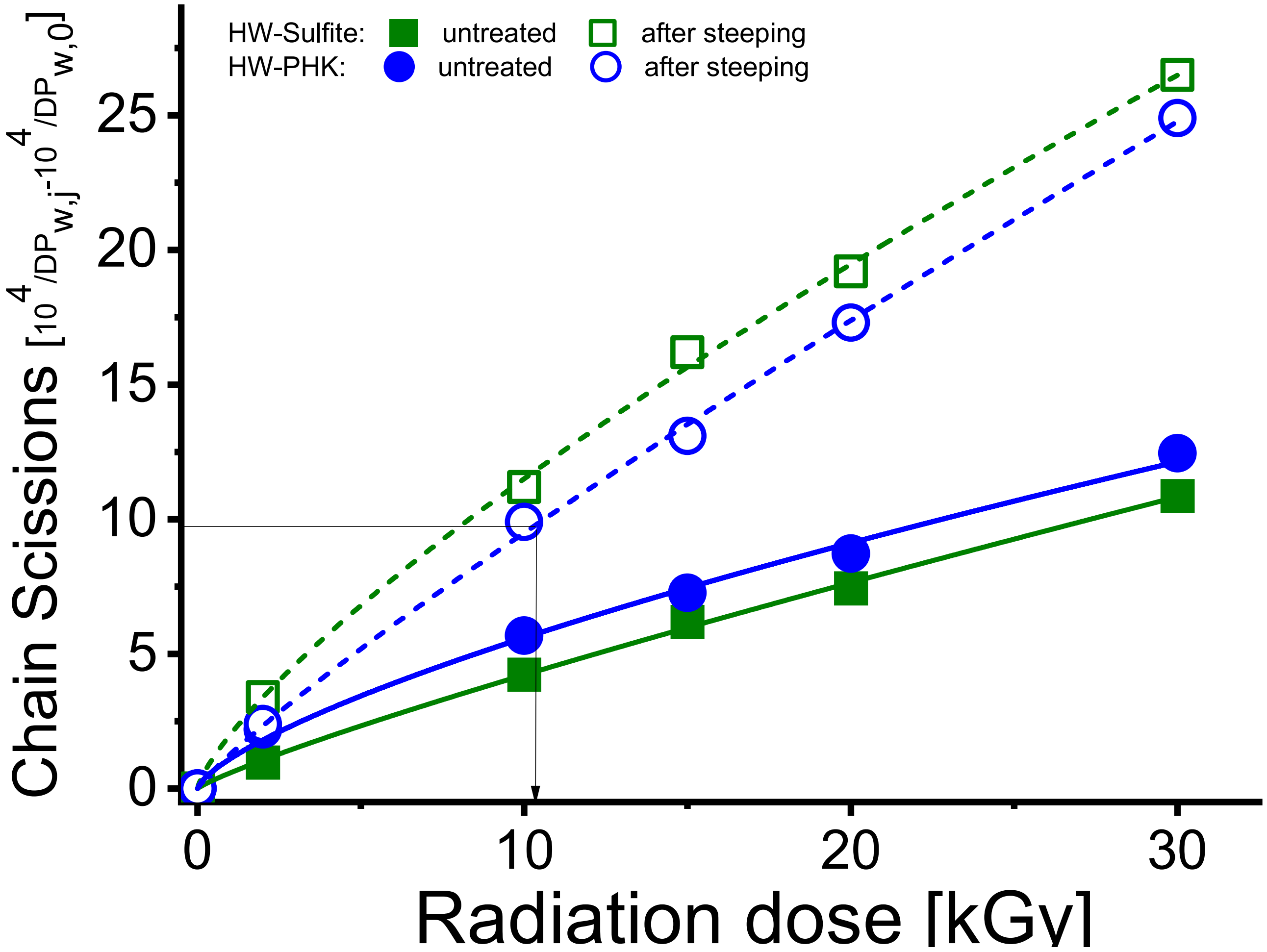

Euca-PHK

$DP_{initial}$ = 1050 (450 mL/g)

DP_{final} = 525 (220 mL/g

CS = $9.54 \cdot 10^{-4}$

Dosage = 10.3 kGy

G = 5.5

$$CS = \left[\frac{10^4}{P_{v,t}} - \frac{10^4}{P_{v,0}}\right] = k_D \cdot D^n$$

Equation from Sakurada

Herbert Sixta (2006)

Advanced Characterization

Quality profile of dissolving pulps

- Presence of Non-Cellulosic Compounds
- Macromolecular Properties
- Functional Groups
- Cell Wall Morphology
- Supramolecular Structure
- Pore Structure, Accessibility
- Reactivity

General Pulp Specification

Pulps	Cell %	Xyl %	GM %	CO mmol/kg	COOH mmol/kg	R18 %	Bright % ISO	Ca ppm	Fe ppm	Si ppm	WRV %
Acid Sulfite (AS)	96.5	3.5	0.7	14	30	94.0	92.5	15	3	20	73
PH-Kraft (PHK)	97.0	2.6	0.0	6	28	97.0	89.0	15	5	20	71
Kraft (K)	84.8	8.0	7.1	15	37	86.7	88.5	15	5	20	84
Cotton Linters (CL)	99.5	0.0	0.0	3	10	99.2	85.0	60	10	10	54

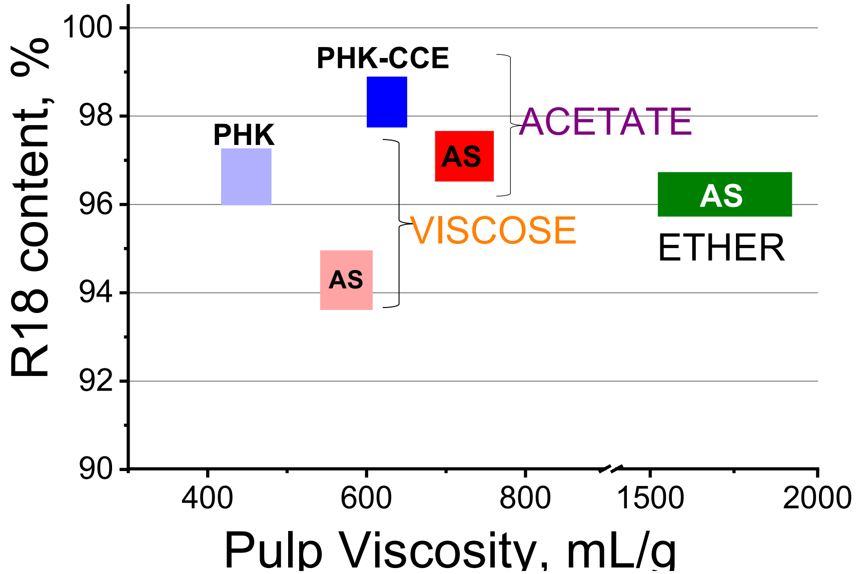

H. Sixta et al., 2005

Molar Mass Distribution

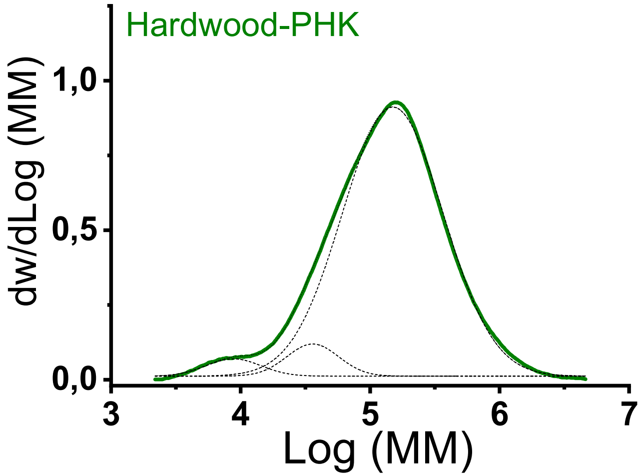

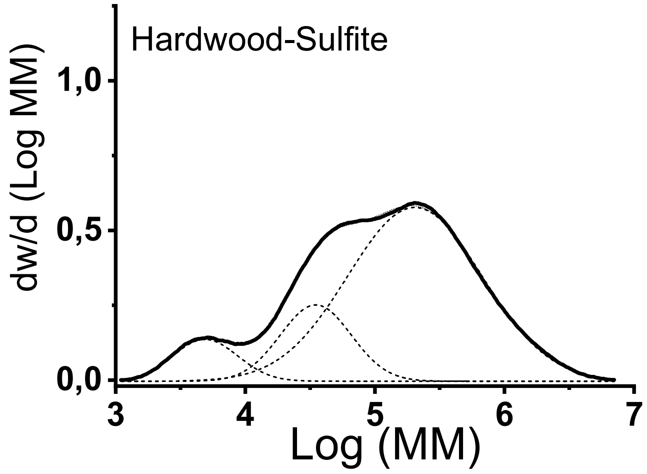

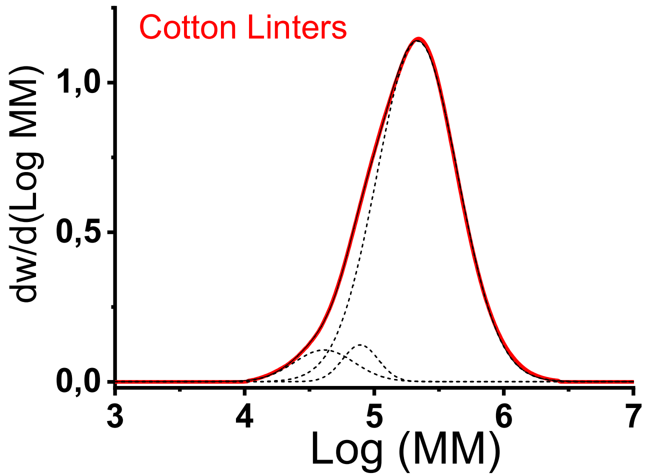

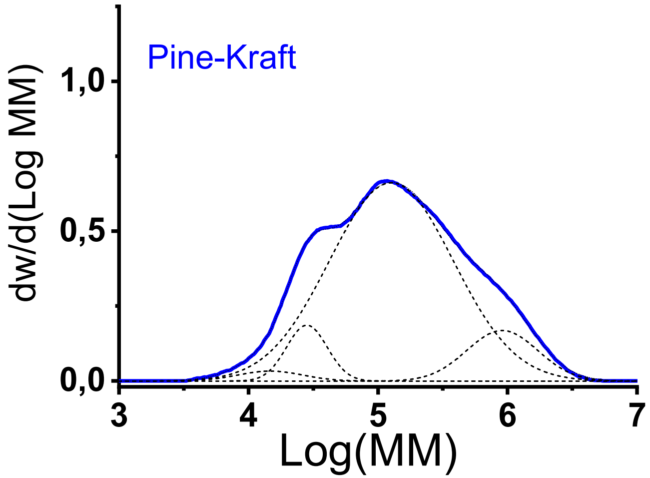

H. Sixta et al., *GPC measurements of commercial DPs*

Pitänen, L.; H. Sixta et al., *Cellulose (2020), 27, 16, 9217-9225*

Effect of MMD on Fiber Work Fracture

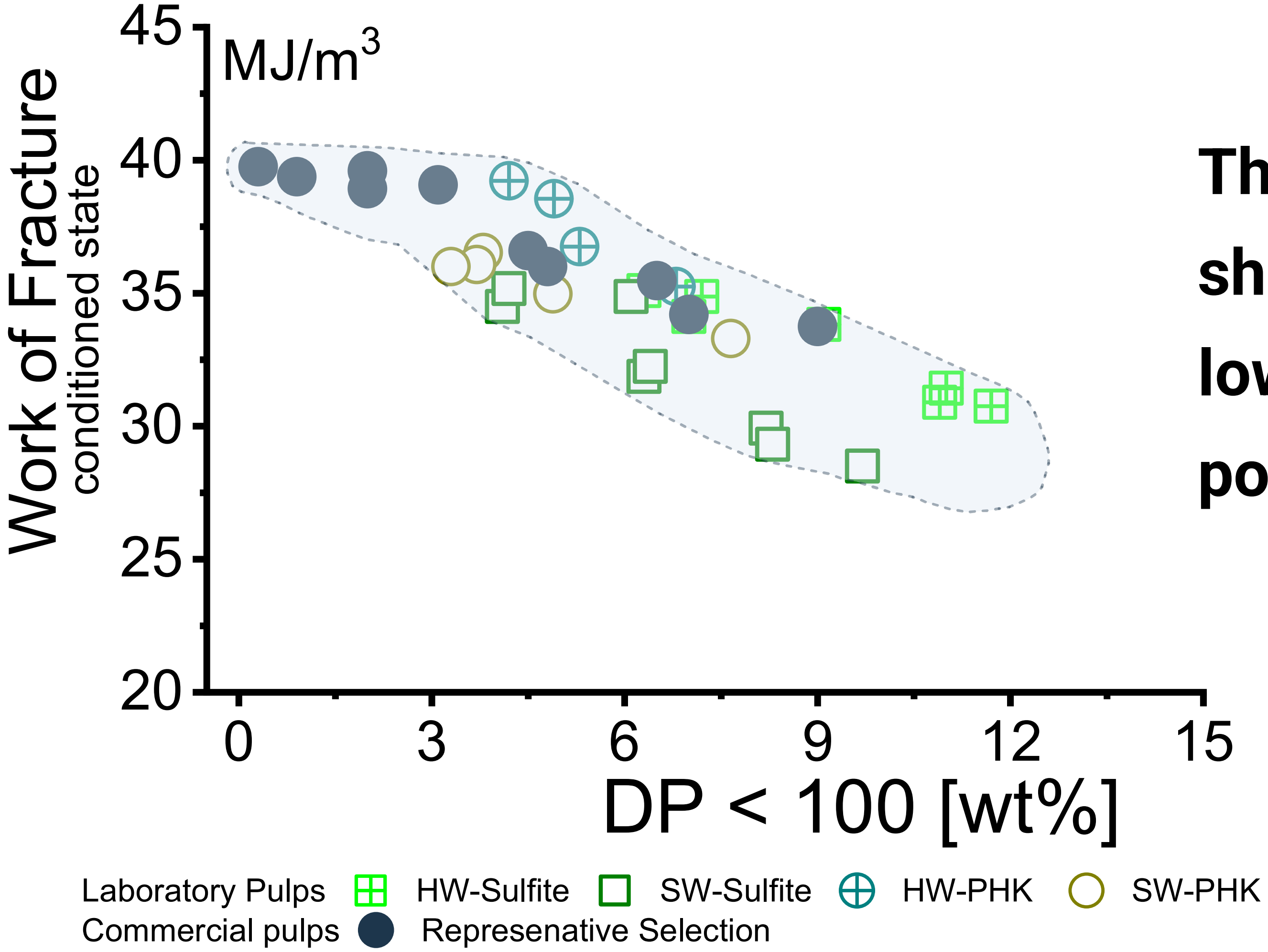

The higher the amount of short chains, DP < 100, the lower is the strength potential of viscose fibers.

H. Sixta et al., *Handbook of Pulp*, 2006

Functional goups

Carbonyl groups occur as reducing endgroups, $\propto \frac{1}{DP_n}$,and along the chain: detrimental in subsequent alkaline treatment and color reversion

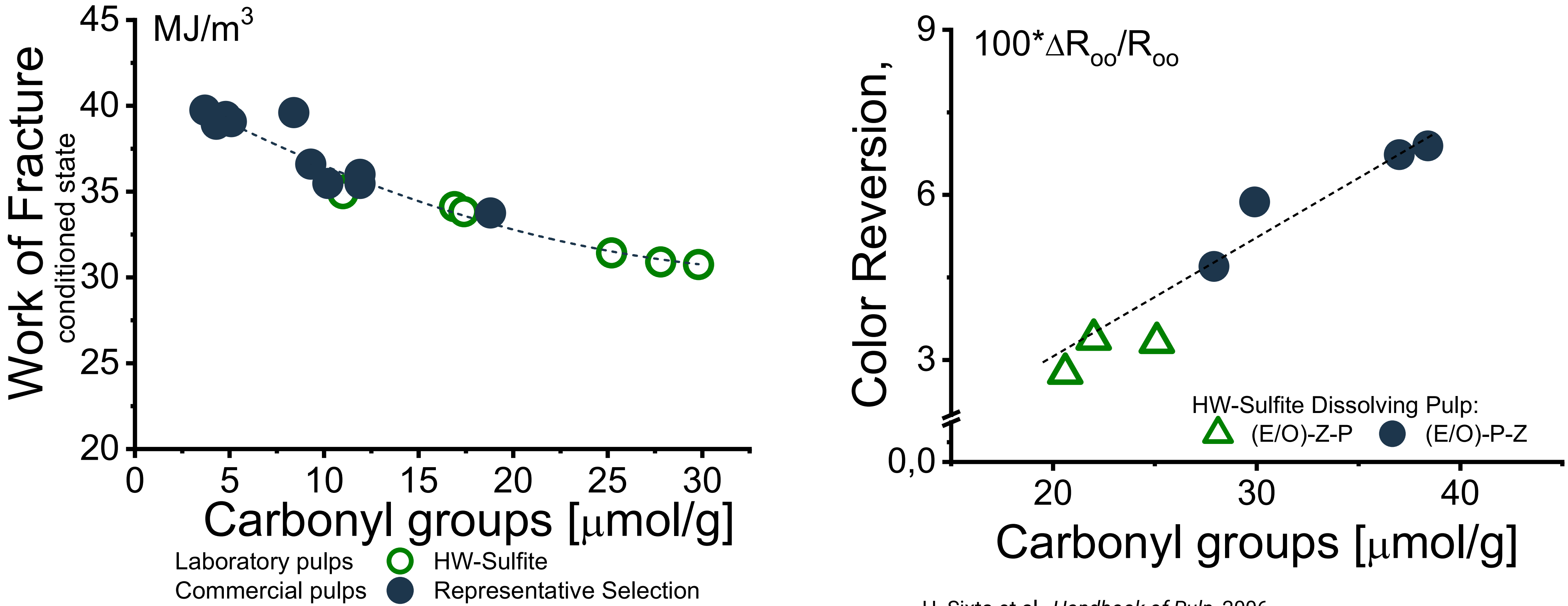

H. Sixta et al., *Handbook of Pulp*, 2006

Hierarchical Cellulose Structure

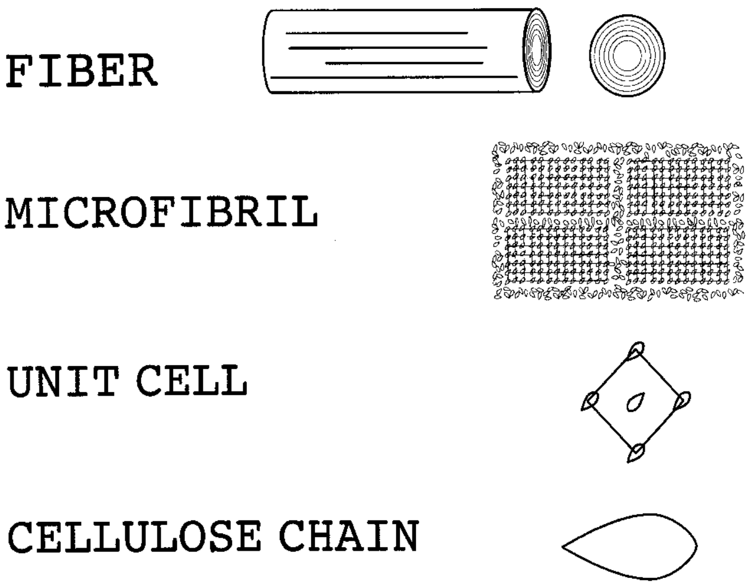

Morphological level
Cell wall architecture, fiber structure

Supramolecular level:
Alignment of cellulose chains

Molecular level:
Individual cellulose chains

Cell Wall Morphology

Microfibrillar Structure

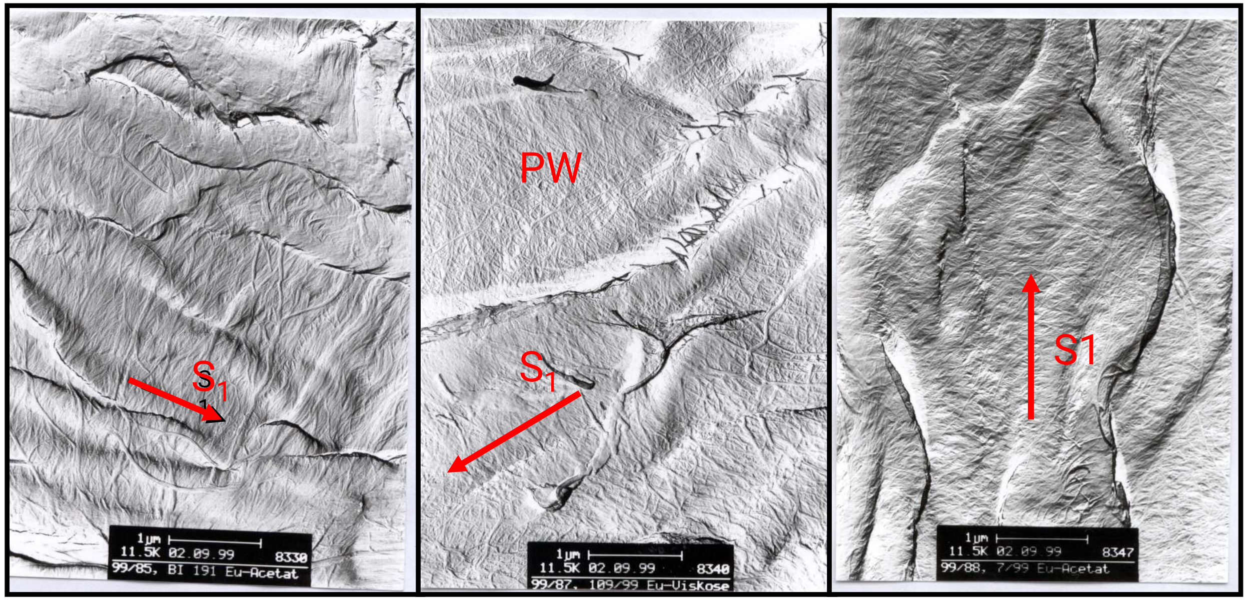

Euca-Sulfite
Dominated by S1-layer

Euca-PHK:
Residues of PW; mild pre-hydrolysis less detrimental to cellulose microfibrils

High-Purity-Euca-PHK:
Intensified pre-hydrolysis further removes PW layers

Sixta, H. Lenzinger Berichte (2000), 79, 119-128.

Crystallite Dimensions

$$L = \frac{K\lambda}{\beta cos\theta}$$

Scherrer equation

L= lateral dimension of a crystallite

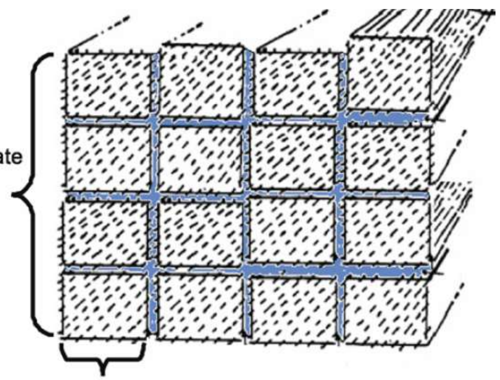

$$X_{fibril} = \frac{I(AS) + I(IAS)}{total\ C - 4\ area\ (NMR)}$$

$$X_{aggregate} = \frac{I(AS)}{total\ C - 4\ area\ (NMR)}$$

Fraction of fibril surface:

$$X = \frac{4 \cdot (n-1)}{n^2}$$

$$n = \frac{2\left(1 + \sqrt{1 - X}\right)}{X}$$

$$L = 0.57n$$

Sometimes instead of X_{fibril}, q_{fibril}

R.H. Newman, Solid State Nuclear Magnetic Resonance 15(1999), 21-29
P.T. Larsson, K. Wickholm, T. Iversen. Carbohydrate Research 302 (1997), 19-25

Crystallite Dimensions with ^{13}C CPMAS NMR

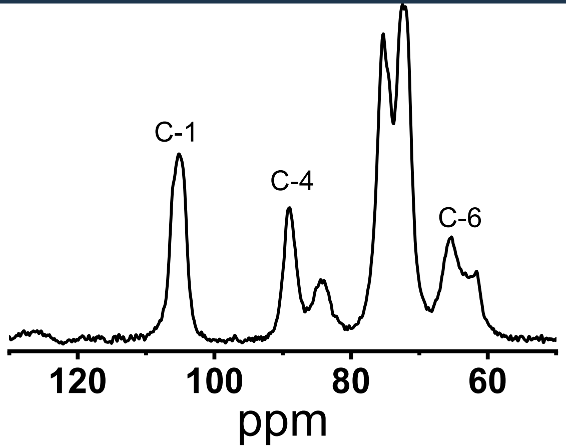

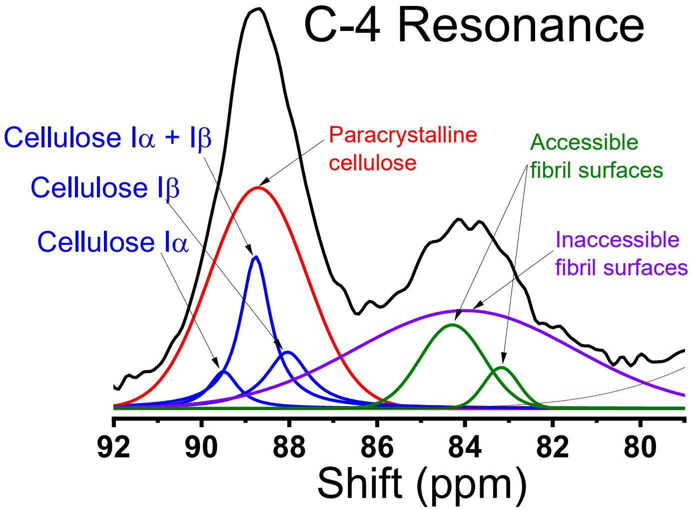

Assignment	**Shift** ppm	**FWHH** Hz	**^{13}C T1** s
Iα	89,42	44	
I(β+b)	88,74	46	
Para-crystalline	88,45	168	138
Iβ	87,87	81	
Accessible fibril surface	84,22	70	18,5
Inaccessible fibril surface	83,38	388	38,8
Accessible fibril surface	83,18	53	11,1
Xylan	81,72	121	

FWWH: full width at half heigth

$CrI = 0.54 \qquad X_{fibril} = 0.46 \qquad X_{aggregate} = 0.11$

$\mathbf{FW = 4.3\ nm}\ (n = 7.54 \rightarrow L = 7.54 \cdot 0.57 = 4.3)$
$\mathbf{AW = 20.2\ nm}\ (n = 35.3 \rightarrow L = 35.3 \cdot 0.57 = 20.2)$

R.H. Newman, Solid State Nuclear Magnetic Resonance 15(1999), 21-29
P.T. Larsson, K. Wickholm, T. Iversen. Carbohydrate Research 302 (1997), 19-25

Viscose Reactivity vs Supramolecular Structure

Pulp	Viscose		CrI (NMR)	FW	AW	Accessible Surface
	FV (g)	Part (ppm)	%	nm	nm	%
Euca K	57	41	52	4,1	22	9,7
Euca K CCE100	49	71	53	4,2	26	8,4
Euca K CCE100 EG	108	23	53	4,2	28	7,9
EK nitren	57	38	57	4,7	20	10,8
PHK	429	18	58	4,8	20	10,8
Acid Sulfite	455	4	53	4,1	19	11,7

No clear relationship between FW and AW and viscose filterability

Wood Sci Technol (2010) 44:533–546

Quality profile of dissolving pulps

- Presence of Non-Cellulosic Compounds
- Macromolecular Properties
- Functional Groups
- Cell Wall Morphology
- Supramolecular Structure
- **Pore Structure, Accessibility**
- **Reactivity**

Pore Structure and Inner Surface

- **Solute exclusion**
- **NMR spectroscopy**
- **Water sorption isotherms, water retetion value (WRV)**
- **Dynamic Vapor Sorption (DVS)**
- **SAXS**
- Thermoporosity (Gibbs-Thompson)
- Cryoporometry (NMR)
- BET: nitrogen absorption
- Mercury-intrusion porosimetry (Powder Technol (2005)160:61)
- Others

Pore volume by ISEC

Inverse Size Exclusion

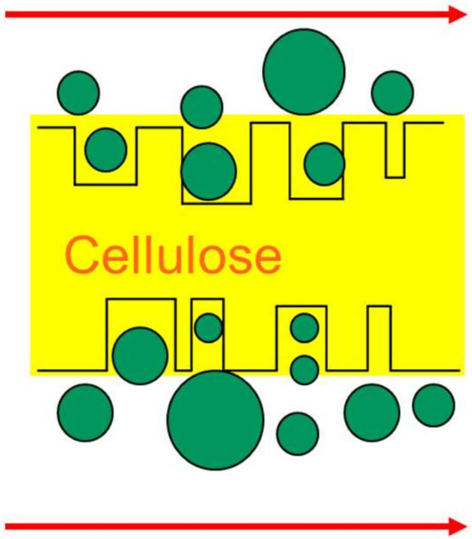

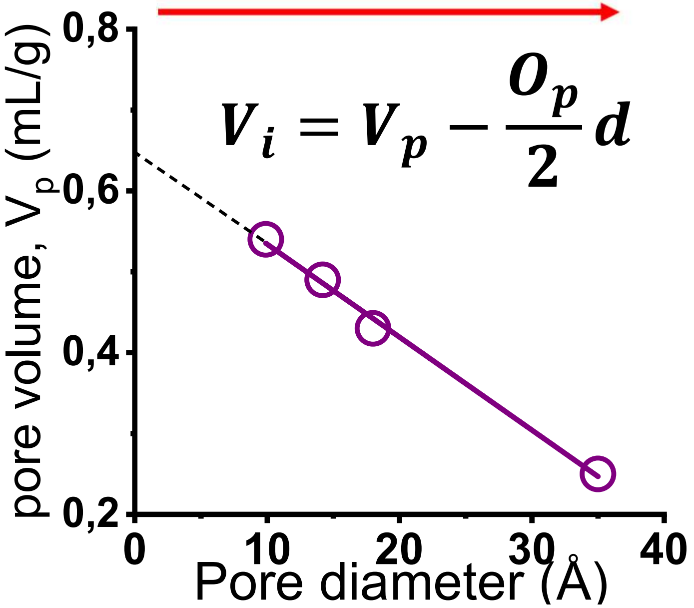

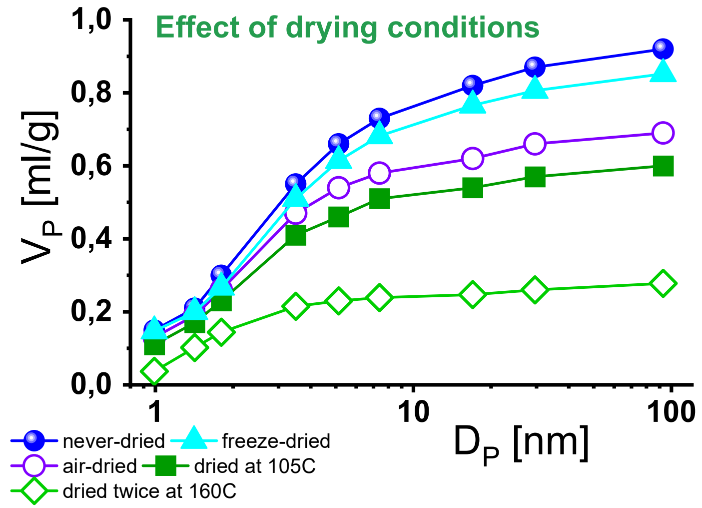

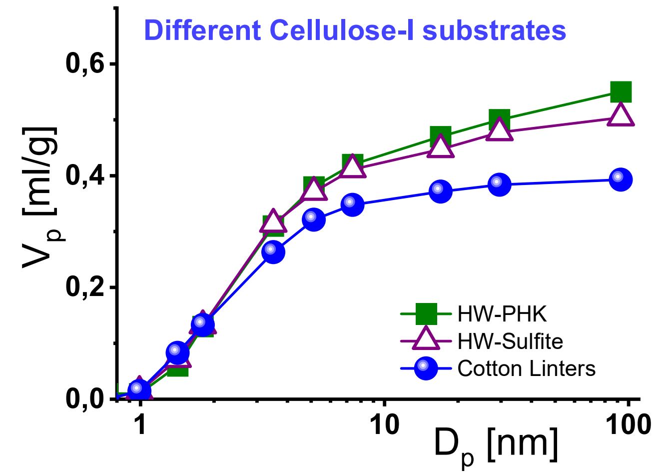

Pulp	V_p	FSP	WRV	D_p	O_p
	mL/g	mL/g	%	nm	m^2/g
HW-S	**0.60**	0.50	73	5.1	235
HW-PHK	**0.65**	0.55	71	5.5	240
CL	**0.45**	0.39	54	4.8	190

Dynamic Water Vapor Sorption

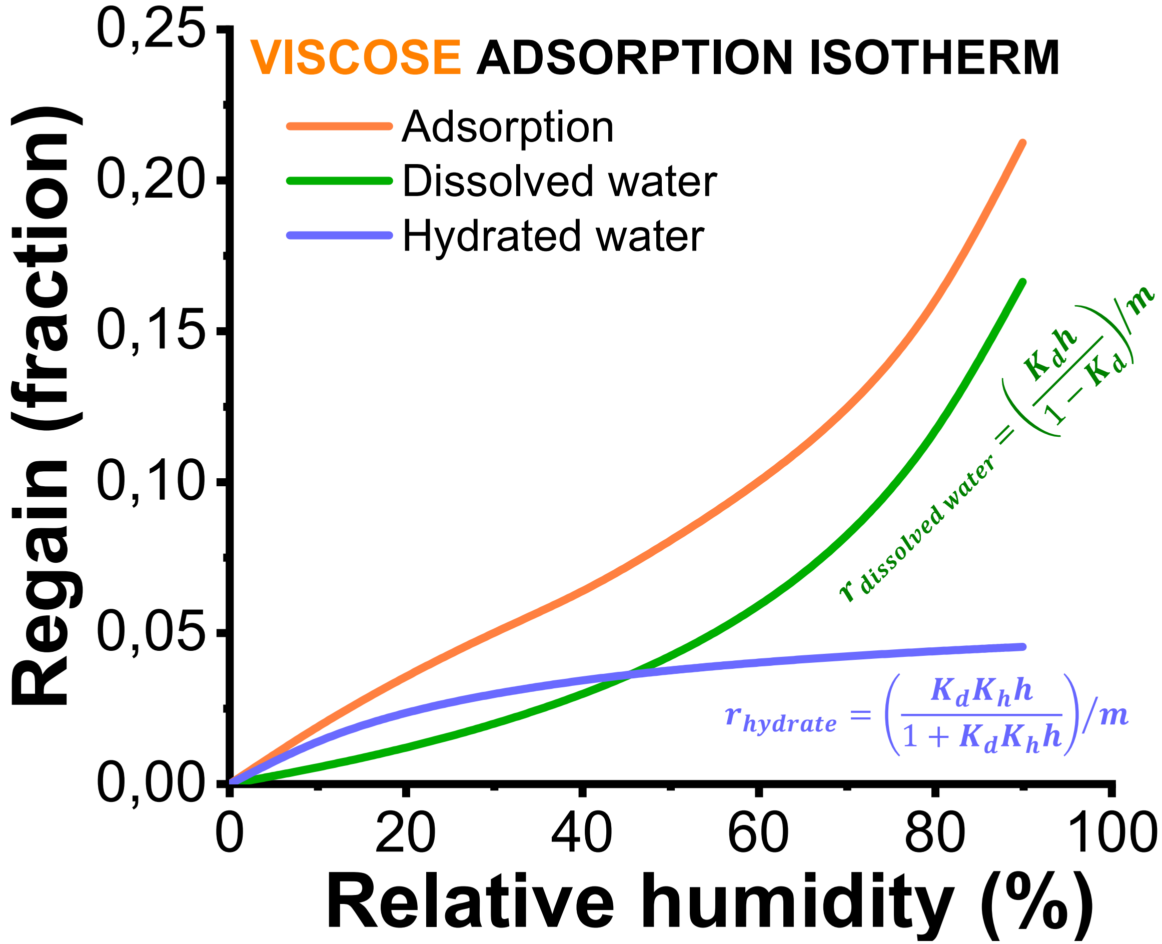

Hailwood-Horrobin Model

h	$rel\ humidity\ (0 \leq h \leq 1)$
r	$regain\ (adsorbed\ water)$
A, B, C	$constants\ derived\ from\ fitting$
m_0	$monolayer\ (ML) coverage$
K_d	$equilibrium\ constant\ of\ the\ ML\ dissolution$
K_h	$equilibrium\ constant\ of\ the\ ML\ hydration$
M	$molar\ mass\ of\ water: 18\ g/mol$
$\Delta G_{h,d}$	$free\ energy\ changes\ referenced\ to\ liquid\ water\ in\ \ J/g$

Hailwood, A.J. and S. Horrobin, *Trans. Faraday Soc.*, 1946. **42B:** p. 84-92, discussion 94-102

Sorption & Desorption Isotherms (DVS)

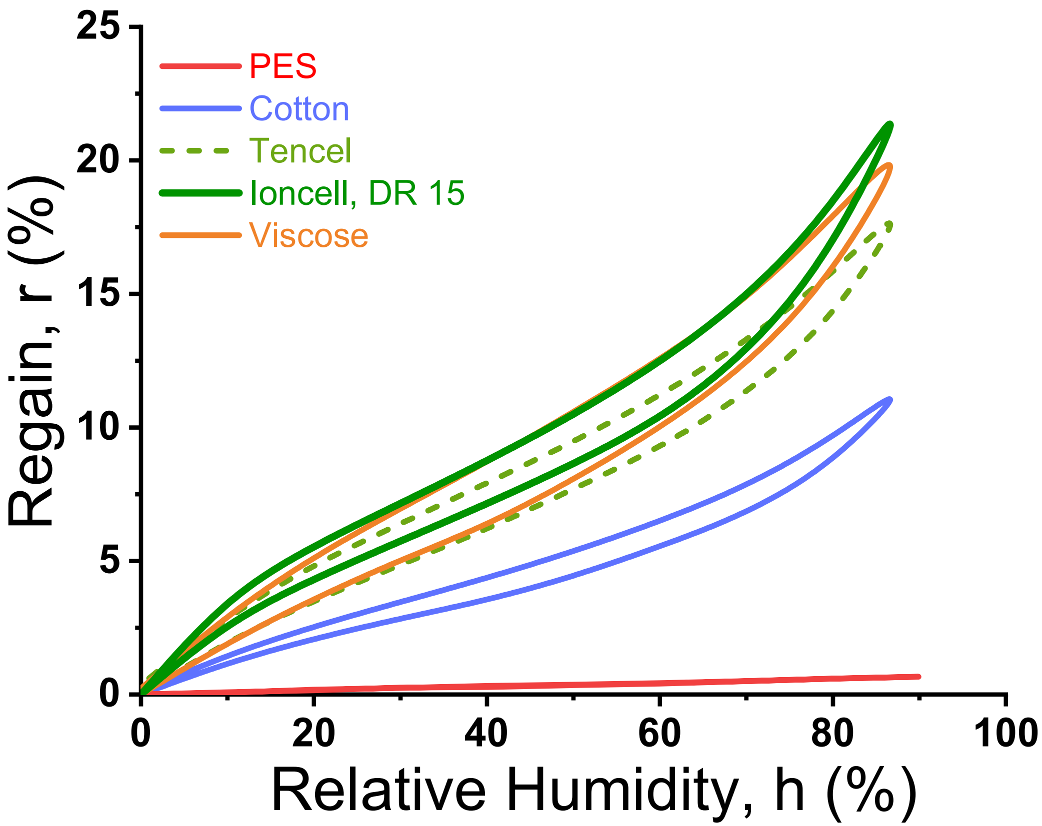

Fits by the **Hailwood-Horrobin** model

$$\frac{h}{r} = A + B \cdot h - C \cdot h^2$$

$$A = 1/[m_0 K_d (K_d + 1)]$$
$$B = (K_h - 1)/[m_0 (K_h + 1)]$$
$$C = K_h K_d/[m_0 (K_h + 1)]$$

$$\Delta G_{h,d} = -\left(\frac{RT}{M}\right) ln(K_{h,d})$$

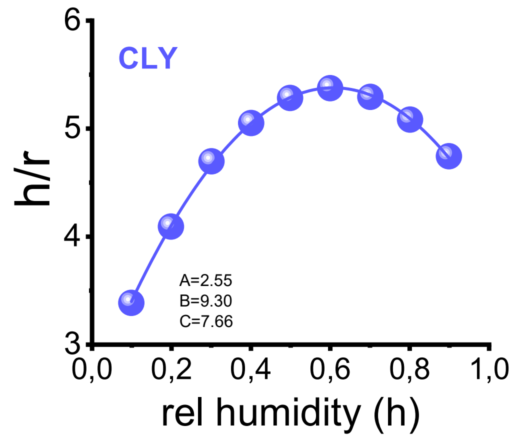

Sample	Sorption	Desorption	Hysteresis*	Sorption	Desorption	Sorption		Desorption	
	Monolayer water			Surface area		ΔG_h	ΔG_d	ΔG_h	ΔG_d
	(g/g)	(g/g)	%	m²/g				J/g	J/g
Cotton fibers	0,0325	0,0431	33	98	129	-213	27	-213	40
PES fibers	0,0041	0,0039	0	12	12	-162	80	-203	78
Tencel, 1.3 dtex	0,0605	0,0777	29	181	233	-199	35	-251	50
Viscose	0,0646	0,0916	42	194	275	-172	31	-219	52
Ioncell, DR 15	0,0578	0,0741	28	173	222	-275	24	-299	35

Hailwood, A.J. and S. Horrobin, *Trans. Faraday Soc.*, 1946. **42B:** p. 84-92, discussion 94-102

Hydration vs Crystallite Width

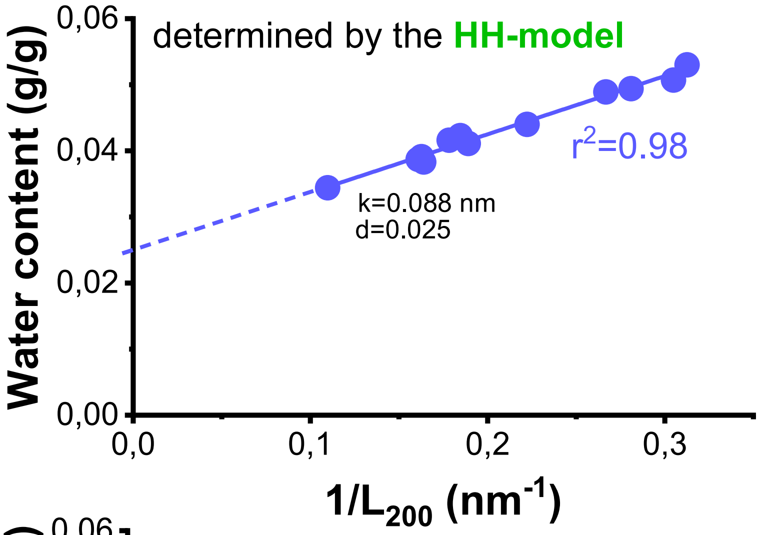

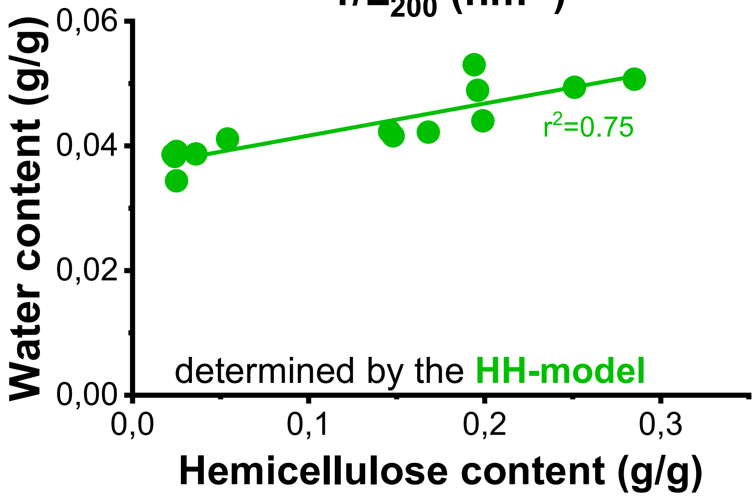

Driemeier, C. and J. Bragatto, J. Phys. Chem. B, 2013. **117** p. 415-421.

Linear relation between monolayer hydration and reciprocal crystallite width theoretically explained by geometric model

ϵ, void from imperfect packing:

$\varepsilon \propto (L + 2\delta)$

v_h ...*volume fraction occupied by hydrated polysaccharides.*

$\textbf{cross} - \textbf{section area} \propto L^2$

$$v_h = \frac{[(L+2\delta)^2 - L^2] + \varepsilon(L+2\delta)^2}{(L+2\delta)^2(1+\varepsilon)}$$

$$v_h \approx \frac{\varepsilon}{\varepsilon+1} + \frac{4\delta}{(1+\varepsilon)}\left(\frac{\mathbf{1}}{\boldsymbol{L}}\right)$$

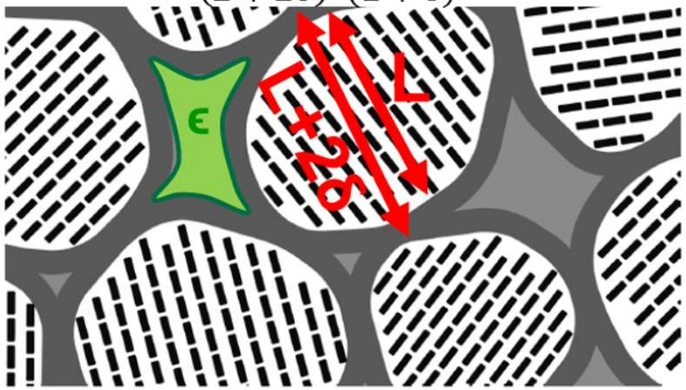

Monolayer water sorption is **structural** (crystallite width) not compositional (hemi)

Void structure determined by SAXS

Two-phase system[1]:

- cellulose/air, the void fraction, w_v, and
- the specific surface O_{sp}

PULPS	W_v %	O_{sp} m^2/cm^3
Euca PH-Kraft Viskose	2,7	1,9
Euca PH-Kraft Acetat	3,8	1,2
Beech Sulfit	2,9	1,7
Euca-Sulfit	2,8	1,3
Euca-PH-Kraft CCE	3,1	1,9

Sixta, H. and A. Borgards. Das Papier, **1999**. **53**(4): p. 220-234.

[1]Porod

Fiber wall pore sizes in water swollen state

Based on solid-state NMR for determining the lateral fibril aggregate dimensions **L**:

$$X = (4n - 4)/n^2;$$

$$\boldsymbol{L = n * 0.57}$$

$$\boldsymbol{\sigma_{sat} = \frac{4}{L \cdot \varrho_s}}$$

$\boldsymbol{\sigma_{sat}}$ .... specific surface area in water-swollen state assuming cylindrical pores, *i.e.*, pore width corresponding to 4V/A

Cellulose (2013) 20:623-631

Fiber wall pore sizes in water swollen state

and FSP (Dextran 2000, R_H=101 nm) measurement

$$FSP = \sigma_{sat} \varrho_L t$$

t… thickness; 2*t = average pore size

$$2t = \frac{2FSP}{\sigma_{sat} \varrho_L}$$

	water-swollen state			
Samples	**FSP**	**a(LFAD)**	**σ_{sat}**	**Av pore size**
	g/g	NMR (nm)	NMR (m^2/g)	2*t (nm)
Cotton Linters	**0,21**	**32,2**	**83**	**5,1**
SW-Sulfite DP	**0,94**	**16,9**	**158**	**11,9**
HW-Sulfite DP	**1,05**	**17,5**	**152**	**13,8**

Cellulose (2013) 20:623-631